AD-A091 540 NAVAL RESEARCH LAB WASHINGTON DC F/G 20/3
MAGNETO-OPTIC MATERIALS FOR BIASING RING LASER GYROS. REPORT NU--ETC(U)
SEP 80 J J KREBS, W G MAISCH
UNCLASSIFIED NRL-MR-4364 NL

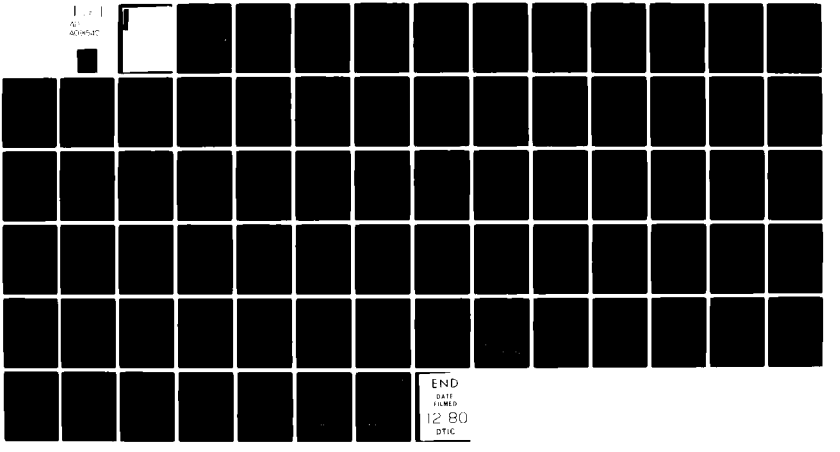

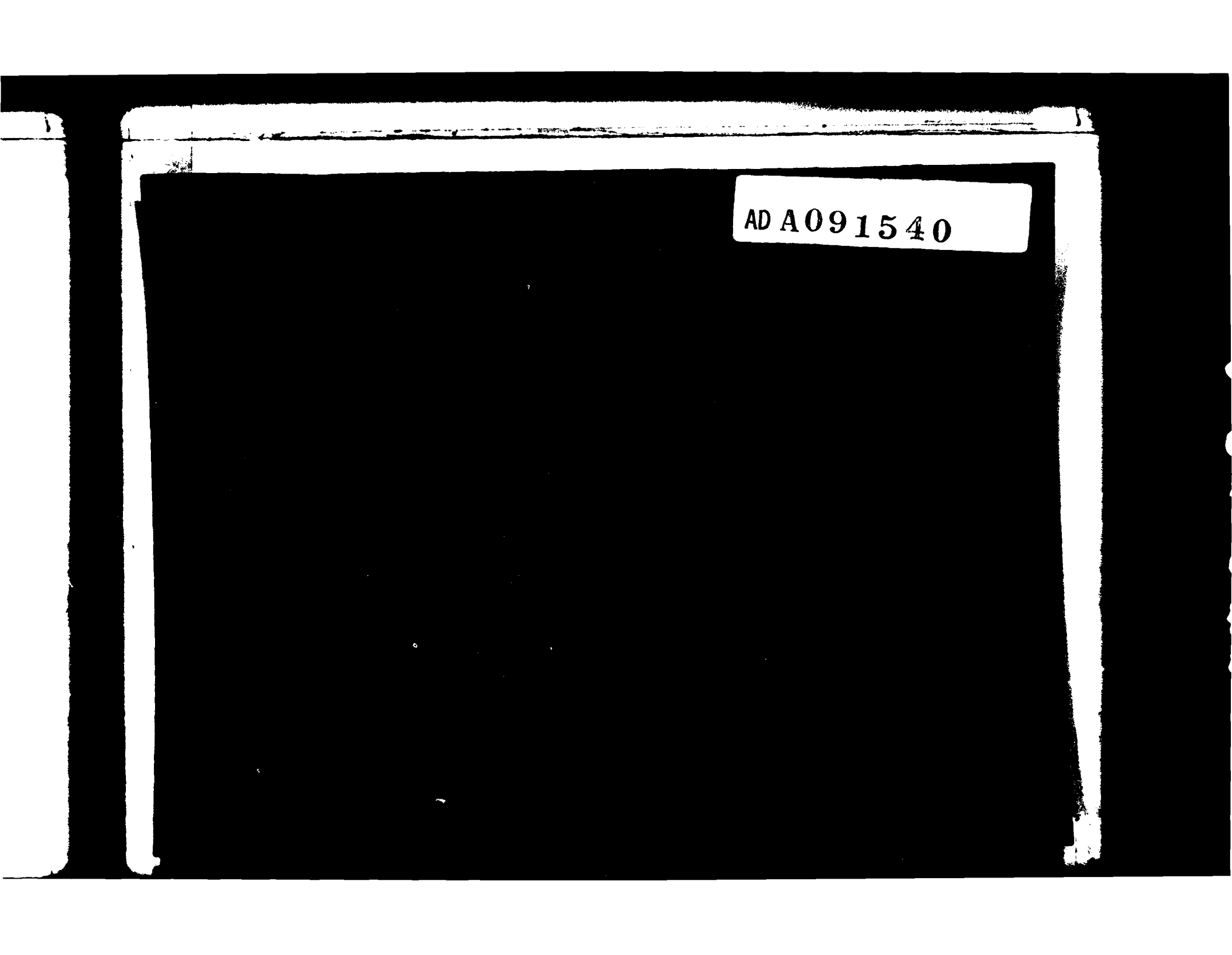

SECURITY CLASSIFICATION OF THIS PAGE (When Data Entered)

REPORT DOCUMENTATION PAGE

READ INSTRUCTIONS BEFORE COMPLETING FORM

1. REPORT NUMBER: NRL Memorandum Report 4364	2. GOVT ACCESSION NO.: AD-A091 540
3. RECIPIENT'S CATALOG NUMBER:	
4. TITLE (and Subtitle): MAGNETO-OPTIC MATERIALS FOR BIASING RING LASER GYROS – REPORT NO. 3 (COMPUTER MODEL FOR EVALUATING SCATTERING FROM MULTI-LAYER DIELECTRIC THIN FILM STRUCTURES CONTAINING A MAGNETIC LAYER)	5. TYPE OF REPORT & PERIOD COVERED: Interim report on a continuing NRL problem
	6. PERFORMING ORG. REPORT NUMBER:
7. AUTHOR(s): J. J. Krebs and W. G. Maisch	8. CONTRACT OR GRANT NUMBER(s):
9. PERFORMING ORGANIZATION NAME AND ADDRESS: Naval Research Laboratory, Washington, DC 20375	10. PROGRAM ELEMENT, PROJECT, TASK AREA & WORK UNIT NUMBERS: 6272N;WF21-234 52-0821-0-0
11. CONTROLLING OFFICE NAME AND ADDRESS: Department of the Navy, Naval Air Systems Command, Washington, DC 20361	12. REPORT DATE: September 30, 1980
	13. NUMBER OF PAGES: 74
14. MONITORING AGENCY NAME & ADDRESS(if different from Controlling Office)	15. SECURITY CLASS. (of this report): UNCLASSIFIED
	15a. DECLASSIFICATION/DOWNGRADING SCHEDULE:

16. DISTRIBUTION STATEMENT (of this Report)

Approved for public release; distribution unlimited.

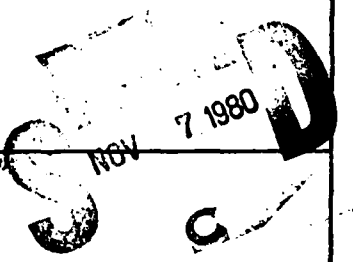

17. DISTRIBUTION STATEMENT (of the abstract entered in Block 20, if different from Report)

18. SUPPLEMENTARY NOTES

This program is supported by NAVAIRSYSCOM through ADPO-35 on Contract N00019-80-WR-01055.

19. KEY WORDS (Continue on reverse side if necessary and identify by block number)

LPS Vol-4
Laser gyros
Magneto-optical materials

20. ABSTRACT (Continue on reverse side if necessary and identify by block number)

A computer model for evaluating the optical and magneto-optical scattering from a multilayer magnetic-dielectric thin film structure is described. The model handles the Faraday effect in the magnetic layer as well as all three magnetic Kerr effects (transverse, polar, and longitudinal) at its interfaces. This model should serve as a useful design tool for magnetic bias ring laser gyro mirrors and typical results are shown for this application.

DD FORM 1 JAN 73 1473 EDITION OF 1 NOV 65 IS OBSOLETE
S/N 0102-014-6601

SECURITY CLASSIFICATION OF THIS PAGE (When Data Entered)

CONTENTS

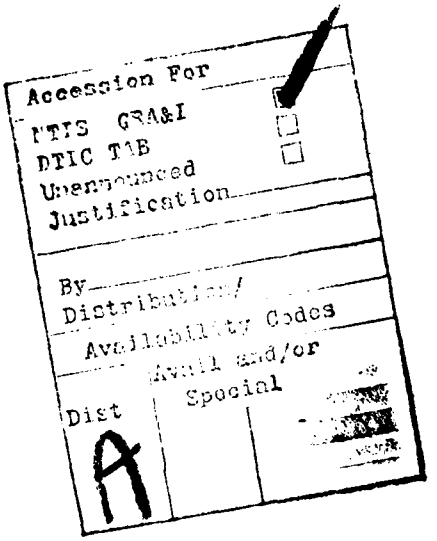

MAGNETO-OPTIC MATERIALS FOR BIASING RING LASER GYROS – REPORT NO. 3 (COMPUTER MODEL FOR EVALUATING SCATTERING FROM MULTI-LAYER DIELECTRIC THIN FILM STRUCTURES CONTAINING A MAGNETIC LAYER)

I. INTRODUCTION AND OVERVIEW

The counterpropagating beams in a ring laser can be employed to sense physical rotation and hence form the basis for a ring laser gyroscope (RLG) [1]. Via the Sagnac effect, the two similar counterpropagating beams oscillate at slightly different frequencies with the difference frequency $\Delta\nu$ given by

$$\Delta\nu = 4A\,\Omega/L\lambda \tag{1}$$

where A is the enclosed area and L the optical length of the RLG, Ω is the rotation rate and λ, the laser optical wavelength. When Ω becomes too small the two beams can lock at a common frequency with consequent loss of rate information. This lock-in problem arises from optical backscatter which couples the beams. As a result, it is important to keep the optical path as free of additional elements as possible.

Because of their non-reciprocal propagation properties, magneto-optical ($M-O$) elements can introduce a controllable frequency difference or magnetic bias $\Delta\nu_b$ and thus avoid the lock-in problem in an elegant manner. The magneto-optical effects which are linear in the magnetization of the material and hence are useful for this application are: (1) the Faraday effect in transmission and (2) the magnetic Kerr effect in reflection. The Kerr effect has three subcases: transverse, polar and longitudinal, depending on how the magnetization is aligned with respect to the plane of the sample and the plane of incidence of the light beams. These $M-O$ effects are discussed in Report No. 1 [2] of this series where it is shown that they each introduce a differential phase shift $\Delta\Phi$ between properly chosen, similar counterpropagating beams. The magnetic bias induced is given by [1]

Manuscript submitted August 25, 1980.

$$\Delta\nu_b = (\Delta\Phi/2\pi)c/L \tag{2}$$

where $\Delta\Phi$ is in radians and c is the velocity of light. A review article on the applications of magneto-optics in ring laser gyroscopes has recently been prepared [3] and provides a concise unified treatment of the subject.

It is advantageous to use the Kerr $M-O$ effects for achieving magnetic bias because then the $M-O$ element can be used as one of the mirrors which define the RLG cavity. This means that it is not necessary to place any additional elements in the beam as would be the case if one used the Faraday effect. As a result the problems related with scattering from extra surfaces are eliminated.

The reflectivity of typical magnetic metal films is only in the range 0.4-0.7 for the He-Ne wavelengths 0.63 μm and 1.15 μm used in RLGs. These low reflectivities are inconsistent with the optical loss requirements of RLGs ($\leqslant$5% at 1.15 μm and $\leqslant$1-2% at 0.63 μm) and with the capabilities of multilayer dielectric (MLD) mirrors which have total optical losses of only 0.02% for laser quality mirrors. In order to reduce the loss associated with the $M-O$ mirror one can overcoat the opaque metallic magnetic layer with an MLD stack which is tuned to be highly reflecting at the wavelength and angle of incidence used. Similarly, if a transparent magnetic material is used, it can be incorporated into an MLD stack, again to achieve adequate reflectivity. RLG mirrors based on both opaque metallic and transparent garnet magnetic films have been discussed by workers at Sperry [4,5].

The above considerations indicate that it is highly desirable to have a unified method of evaluating the important optical and magneto-optical parameters which characterize a given multilayer magnetic-dielectric thin film composite. A computer model which permits various RLG $M-O$ multilayer mirrors to be evaluated and compared quantitatively would be a very useful design tool. With this goal in mind we have produced such a computer model whose characteristics, structure, and details are set forth in the bulk of this report.

In Chapter II the mathematical basis of the method, which is the scattering matrix approach developed by Hunt [6] for multilayer optical structures containing a single magnetic layer, is described. Chapter III shows how these ideas have been incorporated into a computer model (program) which can calculate the differential phase shift, the total reflectivity, the differential reflectivity (for similar counterpropagating beams), and the mode mixing, if any, for a general multilayer structure. All three Kerr effects (transverse, polar and longitudinal) can be handled easily by the model which also takes into account Faraday rotation in the magnetic layer. In Chapter IV, results from calculations on several typical structures which might be used as magnetic bias mirrors in RLG applications are illustrated. Finally, the Fortran listings of the main program and its subroutines are given in the Appendix.

The calculations given in Chapter IV indicate the superiority of mirrors based on magnetic garnets to those based on transition metals such as iron. They also show, however, that MnBi polar Kerr mirrors are a viable alternative to the garnet mirrors. It appears likely that the choice will depend on the cost and reproducibility factors in the fabrication of garnet or MnBi mirrors.

Readers may obtain Fortran versions of the computer program on their flexible disc media by contacting one of the authors at the Naval Research Laboratory, phone number (202)-767-3603.

II. MATHEMATICAL BASIS FOR THE MODEL

A general method of calculation is required if one is to handle a wide variety of multilayer dielectric structures which contain a layer having magneto-optical properties. Fortunately, general scattering matrix methods for evaluating the magneto-optic scattering from such structures were developed in the late 1960's by Smith [7] and Hunt. [6] Our embodiment of the scattering matrix techniques into a computer program possessing a high degree of generality is based on Hunt's methods. In this chapter we first outline the method in enough detail to make our computer program understandable and note an error in Hunt's paper which is corrected in the program used here. That error, in the transverse Kerr Fresnel coefficients $\bar{r}_{pp}$ and $\bar{t}_{pp}$, was pointed out to us by R.E. McClure and the correct derivation can be found in his recent paper [8]. Finally, we write out explicit expressions for the differential phase shift, reflectivity, differential reflectivity, and mode mixing for ring laser gyro $M-O$ mirrors using each of the three Kerr effects.

In Fig. 1 a general thin film structure is shown. It consists of L layers each having a specified thickness d_k and index of refraction n_k. There is a single magnetic layer characterized by d_M, n_M and the magneto-optical coefficient Q. Note that n_M and Q are complex quantities while the other parameters are real.

Let $E_p^{+,k}$ be the total electric vector of a right propagating p-polarized beam at the k interface, in the $k-1$ medium. Similarly, $E_s^{-,k}$ is the total electric vector of a left propagating s-polarized beam at the k interface in the $k-1$ medium. Note that the k interface separates medium $k-1$ from medium k. Then the 4×4 scattering matrix (S^k) which describes the effect of interface k and propagation in the k medium obeys the following equation [6].

$$\begin{bmatrix} E_p^{-,k} \\ E_s^{-,k} \\ E_p^{+,k} \\ E_s^{+,k} \end{bmatrix} = (S^k) \begin{bmatrix} E_p^{-,k+1} \\ E_s^{-,k+1} \\ E_p^{+,k+1} \\ E_s^{+,k+1} \end{bmatrix}. \tag{3}$$

Hunt [6] shows if the k medium has magneto-optical properties then the front-surface scattering matrix (S^M) is given by

$$(S^M) = \begin{bmatrix} [\bar{t}^k - r^k(t^k)^{-1}\bar{r}^k]T_k & r^k(t^k)^{-1}T_k^{-1} \\ -(t^k)^{-1}\bar{r}^k T_k & (t^k)^{-1}T_k^{-1} \end{bmatrix} \tag{4}$$

where r^k, $\bar{r}^k$, t^k and $\bar{t}^k$ are 2 × 2 matrices of Fresnel coefficients. The Fresnel matrices are defined by

$$r^k = \begin{bmatrix} r_{pp}^k & r_{ps}^k \\ r_{sp}^k & r_{ss}^k \end{bmatrix}, \quad \bar{r}^k = \begin{bmatrix} \bar{r}_{pp}^k & \bar{r}_{ps}^k \\ \bar{r}_{sp}^k & \bar{r}_{ss}^k \end{bmatrix} \tag{5}$$

where the Fresnel reflection coefficients at the k interface are r_{ij}^k for an incident beam propagating in the dielectric toward the magnetic medium and are $\bar{r}_{ij}^k$ for an incident beam propagating in the magnetic medium toward the dielectric. Note that p and s refer to the plane of polarization [see Report No. 1, Fig. 2 and Eq. (II-6)] [2]. The t^k and $\bar{t}^k$ matrices contain the corresponding transmission Fresnel coefficients.

In Eq. (2) T_k is a propagation matrix which describes the normal phase retardation and the Faraday effect for a wave ($E_p^{\pm}$, $E_s^{\pm}$) propagating through medium k of thickness d_k. Hunt, based on the work of Robinson, [9] shows that T_k has the form [6]

$$T_k = e^{i\phi_k} \begin{bmatrix} \cos\psi_k & \sin\psi_k \\ -\sin\psi_k & \cos\psi_k \end{bmatrix} \tag{6}$$

where

$$\phi_k = 2\pi n_k d_k \cos\theta_k/\lambda \tag{7}$$

and ψ_k depends on the magneto-optical effect (transverse, longitudinal or polar) with which we are dealing and can be found in Table II. The angle between the beam direction in medium k and the k^{th} interface normal is θ_k. Note that T_k is the same for waves propagating in the right and left directions. When the last layer L is opaque, or is of indefinite (but large) thickness, or if propagation effect for this layer are otherwise not important, one can set $d_L = 0$. This converts T_L into a unit matrix and eliminates the propagation effects while keeping the interface effects. Since $n_k = n_m$ is complex, so is ϕ_k (plus θ_k and ψ_k). This takes into account optical absorption in the magnetic medium.

The Fresnel coefficients for a $M-O$ material in each of the $M-O$ modes are derived by Hunt and we give these expressions for r_{ij}^k, $\bar{r}_{ij}^k$, t_{ij}^k and $\bar{t}_{ij}^k$ and ψ_k in Tables I and II. As can be seen, the Fresnel coefficients for the k interface involve n_{k-1}, n_k, θ_{k-1}, θ_k and Q. We point out that all off-diagonal components of r^k, $\bar{r}^k$, t^k and $\bar{t}^k$ are proportional to Q (or all vanish for the transverse mode). Since $|Q| << 1$, one can neglect second order terms in Q. This means, for example, that

$$(t)^{-1} = \begin{bmatrix} t_{pp} & t_{ps} \\ t_{sp} & t_{ss} \end{bmatrix}^{-1} \cong \begin{bmatrix} 1/t_{pp} & -t_{ps}/t_{pp}t_{ss} \\ -t_{sp}/t_{pp}t_{ss} & 1/t_{ss} \end{bmatrix} \tag{8}$$

where we have suppressed the superscript k.

Table I. Single-Interface Diagonal Fresnel Coefficients

Element	Longitudinal and Polar	Transverse
r_{pp}	$\dfrac{n_2c_1 - n_1c_2}{n_2c_1 + n_1c_2}$	$\dfrac{n_2c_1(1 + iQs_2/c_2) - n_1c_2}{n_2c_1(1 + iQs_2/c_2) + n_1c_2}$
r_{ss}	$\dfrac{n_1c_1 - n_2c_2}{n_1c_1 + n_2c_2}$	$\dfrac{n_1c_1 - n_2c_2}{n_1c_1 + n_2c_2}$
t_{pp}	$(n_1/n_2)(1 + r_{pp})$	$(n_1/n_2)(1 + r_{pp})$
t_{ss}	$1 + r_{ss}$	$1 + r_{ss}$
$\bar{r}_{pp}$	$-r_{pp}$	$-\dfrac{n_2c_1 - n_1c_2(1 + iQs_2/c_2)}{n_2c_1 + n_1c_2(1 - iQs_2/c_2)}$
$\bar{r}_{ss}$	$-r_{ss}$	$-r_{ss}$
$\bar{t}_{pp}$	$(n_2/n_1)(1 - r_{pp})$	$(n_2/n_1)(1 + \bar{r}_{pp})$
$\bar{t}_{ss}$	$1 - r_{ss}$	$1 - r_{ss}$
ϕ	$2\pi d_2 n_2 c_2/\lambda$	$2\pi d_2 n_2 c_2/\lambda$

n_1, n_2 — refractive indices of the dielectric and magnetic media, respectively.

c_1, c_2 — direction cosines for the angle of refraction in the dielectric and magnetic media, respectively.

s_2 — sine of the refraction angle in the magnetic medium.

TABLE II. Single-Interface Off-Diagonal Fresnel Coefficients

Element	Polar	Longitudinal
r_{sp}	$\frac{i}{4} Q t_{pp} t_{ss} s_1/(c_1 s_2)$	$\frac{i}{4} Q t_{pp} t_{ss} s_1/(c_1 c_2)$
r_{ps}	r_{sp}	$-r_{sp}$
t_{sp}	r_{sp}	r_{sp}
t_{ps}	$(n_1/n_2) r_{ps}(1 - 2c_1 c_2/t_{pp})$	$(n_1/n_2) r_{ps}(1 + 2c_1 c_2/t_{pp})$
$\bar{r}_{sp}$	$-r_{pp} r_{sp}/t_{pp}$	$-r_{pp} r_{sp}/t_{pp}$
$\bar{r}_{ps}$	$-r_{ss} t_{ps}/t_{ss}$	$-r_{ss} t_{ps}/t_{ss}$
$\bar{t}_{sp}$	$-r_{pp} r_{sp}/t_{pp}$	$-r_{pp} r_{sp}/t_{pp}$
$\bar{t}_{ps}$	$-r_{ss} r_{ps}/t_{ss}$	$-r_{ss} r_{ps}/t_{ss}$
ψ	$\pi d_2 n_2 Q/\lambda$	$\pi d_2 n_2 Q (s_2/c_2)/\lambda$

n_1, n_2 — refractive indices of the dielectric and magnetic media respectively.
c_1, $c_2 (s_1, s_2)$ — cosine (sine) of the refraction angle in the dielectric and magnetic media, respectively.

One can now write out explicit expressions for $(S^M)_{\text{polar}}$, $(S^M)_{\text{long}}$ and $(S^M)_{\text{trans}}$ and these are given in Tables III and IV. Note that $(S^M)_{\text{polar}}$ and $(S^M)_{\text{long}}$ have the same form while $(S^M)_{\text{trans}}$ is simpler because of the lack of mode mixing in the transverse mode. In Table III, terms of the form $Q \sin \phi_k$ have been neglected as being of order Q^2. Although this approximation could be invalid for a thick transparent $M-O$ slab, we anticipate that $\psi_k << 1$ for practical ring laser gyro applications and hence the approximation is valid.

TABLE III. Front Surface Magneto-Optical Scattering Matrix — Polar and Longitudinal Kerr Effects

$$(S^M) = \begin{bmatrix} \Phi c/t_{pp} & \Phi s/t_{pp} & r_{pp}c/(t_{pp}\Phi) & [(t_{pp}r_{ps} - t_{ps}r_{pp})c/(t_{pp}t_{ss}) - r_{pp}s/t_{pp}]/\Phi \\ -\Phi s/t_s & \Phi c/t_{ss} & (r_{sp}c + r_{ss}t_{pp}s)/(t_{pp}t_{ss}\Phi) & r_{ss}c/(t_{ss}\Phi) \\ \Phi r_{pp}c/t_{pp} & \Phi r_{pp}s/t_{pp} & c/(t_{pp}\Phi) & -(t_{ps}c + t_{ss}s)/(t_{pp}t_{ss}\Phi) \\ -\Phi r_{ss}s/t_{ss} & \Phi r_{ss}c/t_{ss} & (t_{pp}s - t_{sp}c)/(t_{pp}t_{ss}\Phi) & c/(t_{ss}\Phi) \end{bmatrix}$$

$\Phi = e^{i\phi}$, $c = \cos\psi$, $s = \sin\psi$
The superscript $k(=M)$ has been dropped on the Fresnel coefficients as well as on ϕ and ψ.

TABLE IV. Front Surface Magneto-Optical Scattering Matrix — Transverse Kerr Effect

$$(S^M) = \begin{bmatrix} (t_{pp}\bar{t}_{pp} - r_{pp}\bar{r}_{pp})\Phi/t_{pp} & 0 & r_{pp}/(t_{pp}\Phi) & 0 \\ 0 & \Phi/t_{ss} & 0 & r_{ss}/(t_{ss}\Phi) \\ -\bar{r}_{pp}\Phi/t_{pp} & 0 & 1/(t_{pp}\Phi) & 0 \\ 0 & r_{ss}\Phi/t_{ss} & 0 & 1/(t_{ss}\Phi) \end{bmatrix}$$

$\Phi = e^{i\phi}$
The superscript $k(=M)$ has been dropped on the Fresnel coefficient as well as on ϕ.

In order to obtain the back-surface scattering matrix (S^{M+1}), one must reverse the roles of r^k and t^k with respect to $\bar{r}^k$ and $\bar{t}^k$. Furthermore, because of the orientation of the magnetization vector with respect to the front and back surface normals, we must make the substitutions

$$r(Q) \to \bar{r}(-Q), \quad \bar{r}(Q) \to r(-Q)$$
$$t(Q) \to \bar{t}(-Q), \quad \bar{t}(Q) \to t(-Q)$$

for the polar and transverse cases. For the longitudinal case this sign reversal does not occur and we have

$$r(Q) \to \bar{r}(Q), \text{ etc.}$$

Upon making these substitutions in Tables III and IV we get the back-surface results shown in Tables V and VI.

TABLE V. Back Surface Magneto-Optical Scattering Matrix — Polar and Longitudinal Kerr Effects

$$(S^{M+1}) = \begin{bmatrix} \Phi/\bar{t}_{pp} & -G\Phi\tau_{pp}/(\Delta_{ss}\bar{t}_{pp}) & \bar{r}_{pp}/(\bar{t}_{pp}\Phi) & -G\bar{r}_{ss}\tau_{pp}/(\Delta_{ss}\bar{t}_{pp}\Phi) \\ -G\Phi\tau_{ss}/(\Delta_{pp}\bar{t}_{ss}) & \Phi/\bar{t}_{ss} & -G\bar{r}_{pp}\tau_{ss}/(\Delta_{pp}\bar{t}_{ss}\Phi) & \bar{r}_{ss}/(\bar{t}_{ss}\Phi) \\ \Phi\bar{r}_{pp}/\bar{t}_{pp} & G\Phi r_{ps}/(\Delta_{ss}\bar{t}_{pp}) & 1/(\bar{t}_{pp}\Phi) & G\bar{r}_{ss}r_{ps}/(\Delta_{ss}\bar{t}_{pp}\Phi) \\ G\Phi r_{sp}/(\Delta_{pp}\bar{t}_{ss}) & \Phi\bar{r}_{ss}/\bar{t}_{ss} & G\bar{r}_{pp}r_{sp}/(\Delta_{pp}\bar{t}_{ss}\Phi) & 1/(\bar{t}_{ss}\Phi) \end{bmatrix}$$

$\Phi = e^{i\phi}$
The superscript $k(=M+1)$ has been dropped on the Fresnel coefficients and ϕ.
$\Delta_{ss} = 1-(\bar{r}_{ss})^2$, $\Delta_{pp} = 1-(\bar{r}_{pp})^2$
$\tau_{ss} = (\bar{t}_{ss}t_{sp} - \bar{r}_{ss}r_{sp})$, $\tau_{pp} = (\bar{t}_{pp}t_{ps} - \bar{r}_{pp}r_{ps})$
$G = +1$ (Polar), $G = -1$ (Longitudinal)

TABLE VI. Back Surface Magneto-Optical Scattering Matrix — Transverse Kerr Effect

$$(S^{M+1}) = \begin{bmatrix} [t_{pp}(-Q)\bar{t}_{pp}(-Q) - r_{pp}(-Q)\bar{r}_{pp}(-Q)]\Phi/\bar{t}_{pp}(-Q) & 0 & \bar{r}_{pp}(-Q)/[\bar{t}_{pp}(-Q)\Phi] & 0 \\ 0 & \Phi/\bar{t}_{ss} & 0 & \bar{r}_{ss}/(\bar{t}_{ss}\Phi) \\ -r_{pp}(-Q)\Phi/\bar{t}_{pp}(-Q) & 0 & 1/[\bar{t}_{pp}(-Q)\Phi] & 0 \\ 0 & \bar{r}_{ss}\Phi/\bar{t}_{ss} & 0 & 1/(\bar{t}_{ss}\Phi) \end{bmatrix}$$

$\Phi = e^{i\phi}$
The superscript $k\ (= M+1)$ has been dropped on the Fresnel coefficients and ϕ.

Finally, we note that if we are dealing with an interface at which both media are nonmagnetic dielectrics, then Eq. (5) reduces to the simple form

$$(S^k)_{\text{diel}} = \begin{bmatrix} \Phi^k/t_{pp}^k & 0 & r_{pp}^k/(t_{pp}^k\Phi^k) & 0 \\ 0 & \Phi^k/t_{ss}^k & 0 & r_{ss}^k/(t_{ss}^k\Phi^k) \\ \Phi^k r_{pp}^k/t_{pp}^k & 0 & 1/(t_{pp}^k\Phi^k) & 0 \\ 0 & \Phi^k r_{ss}^k/t_{ss}^k & 0 & 1/(t_{ss}^k\Phi^k) \end{bmatrix} \tag{9}$$

where $\Phi^k = e^{i\phi_k}$ and the Fresnel coefficients can be obtained from Table I with $Q = 0$.

The overall scattering matrix for the general multilayer magnetic-dielectric thin-film structure shown in Fig. 1 is then

$$(S) = (S^1)(S^2) \cdots (S^M)(S^{M+1}) \cdots (S^{L-1})(S^L) \tag{10}$$

in which all but (S^M) and (S^{M+1}) are dielectric-dielectric matrices of the form Eq. (7). Thus we have

$$\begin{bmatrix} E_p^{-,0} \\ E_s^{-,0} \\ E_p^{+,0} \\ E_s^{+,0} \end{bmatrix} = (S) \begin{bmatrix} E_p^{-,L} \\ E_s^{-,L} \\ E_p^{+,L} \\ E_s^{+,L} \end{bmatrix}. \tag{11}$$

The scattering matrix (S) contains all the desired information about the optical and magneto-optical properties of the multilayer structure. One can obtain the Fresnel reflection and transmission coefficients for the entire stack as well as the Kerr rotations K_p and K_s and Faraday rotations F_p and F_s. (All of these quantities, like the components of (S), are in general complex numbers.) The equations which relate these stack Fresnel and rotation parameters to the components of (S) are derived by Hunt [6] and are summarized in Table VII.

TABLE VII. Fresnel Coefficients for Entire Stack

R_{pp}	$= (S_{44}S_{13} - S_{14}S_{43})/(S_{33}S_{44} - S_{34}S_{43})$
R_{ss}	$= (S_{23}S_{34} - S_{24}S_{33})/(S_{34}S_{43} - S_{33}S_{44})$
R_{ps}	$= (S_{34}S_{13} - S_{14}S_{33})/(S_{34}S_{43} - S_{33}S_{44})$
R_{sp}	$= (S_{23}S_{44} - S_{24}S_{43})/(S_{33}S_{44} - S_{34}S_{43})$
$\tan K_p$	$= R_{sp}/R_{pp} \quad \tan K_s = R_{ps}/R_{ss}$
T_{pp}	$= S_{44}/(S_{33}S_{44} - S_{34}S_{43})$
T_{ss}	$= S_{33}/(S_{33}S_{44} - S_{34}S_{43})$
T_{ps}	$= -S_{34}/(S_{33}S_{44} - S_{34}S_{43})$
T_{sp}	$= -S_{43}/(S_{33}S_{44} - S_{34}S_{43})$
$\tan F_p$	$= T_{sp}/T_{pp} \quad \tan F_s = T_{ps}/T_{ss}$

The ring laser gyro supports counterpropagating models of the same polarization(s). The desired optical and magneto-optical characteristics of a magnetic-dielectric multilayer structure are: 1) the differential phase shift $\Delta\Phi$ between similar counterpropagating beams, 2) the reflectivity R of the stack for these beams, 3) the differential reflectivity ΔR, 4) the figure of merit $FM \equiv \Delta\Phi/(1-R)$, and 5) the mode mixing $\epsilon \equiv$ ratio of the improper to the desired polarization amplitudes. Since the p and s polarizations are eigenmodes in the transverse case, $\epsilon \equiv 0$ for transverse $M-O$ Kerr mirrors. We now consider each of the $M-O$ cases in turn.

A. Transverse Kerr Effect

1) Differential Phase shift

$$\begin{aligned}\Delta\Phi_T &\equiv Arg\{E_p^-(Q)\} - Arg\{E_p^-(-Q)\} \\ &= Arg\{R_{pp}(Q)\} - Arg\{R_{pp}(-Q)\}\end{aligned} \tag{12}$$

where $Arg\{X\}$ means the argument of the complex quantity X and the R_{ij} are the reflection Fresnel coefficients for the entire stack (obtained from the S_{ij} via Table VII). We have used the fact that the magnetization (and Q) looks reversed to the two counterpropagating p-polarized beams.

2) Reflectivity

$$|R_{pp}(0)|^2 = \frac{1}{2}\{|R_{pp}(Q)|^2 + |R_{pp}(-Q)|^2\} \tag{13}$$

3) Differential Reflectivity

$$\Delta R_T \equiv (|R_{pp}(Q)|^2 - |R_{pp}(-Q)|^2/|R_{pp}(0)|^2. \tag{14}$$

The calculation of FM_T is obvious and $\epsilon_T \equiv 0$.

B. Polar Kerr Effect

It is more natural to deal with circularly polarized beams in this case so we use the circular Fresnel coefficients for the stack, viz. R_{RR}, R_{LL}, R_{LR} and R_{RL}. It is easy to show that these can be expressed in terms of the R_{pp}, etc. as follows.

$$\begin{bmatrix} R_{RR} & R_{RL} \\ R_{LR} & R_{LL} \end{bmatrix} = \frac{1}{2} \begin{bmatrix} (R_{pp} + R_{ss} - iR_{ps} + iR_{sp}) & (R_{pp} - R_{ss} + iR_{ps} + iR_{sp}) \\ (R_{pp} - R_{ss} - iR_{ps} - iR_{sp}) & (R_{pp} + R_{ss} + iR_{ps} - iR_{sp}) \end{bmatrix}. \tag{15}$$

Since $R_{ss} \simeq -R_{pp}$ and $R_{ps} \simeq R_{sp}$, we see that $|R_{RR}|, |R_{LL}| << |R_{RL}|, |R_{LR}|$, i.e., for the most part $R \rightarrow L$ and $L \rightarrow R$ upon reflection. However, since R_{RR} and $R_{LL} \neq 0$, there is mode mixing and induced ellipticity.

1) Differential Phase shift

$$\begin{aligned} \Delta\Phi_p &\equiv Arg\{E_R^-\}_{L^+in} - Arg\{E_L^-\}_{R^+in} \\ &= Arg\{R_{RL}\} - Arg\{R_{LR}\} \end{aligned} \tag{16}$$

2) Reflectivity

$$\begin{aligned} |R_{RL}(0)|^2 &= |R_{LR}(0)|^2 \\ &= \frac{1}{4} |R_{pp}(0) - R_{ss}(0)|^2 \end{aligned} \tag{17}$$

3) Differential Reflectivity

$$\Delta R_p = (|R_{LR}|^2 - |R_{RL}|^2)/|R_{RL}(0)|^2 \tag{18}$$

4) Mode Mixing

$$\epsilon_{PR} = |R_{RR}/R_{LR}| \tag{19a}$$

$$\epsilon_{PL} = |R_{LL}/R_{RL}|. \tag{19b}$$

A ring laser gyro using a polar Kerr effect $M-O$ mirror must have an even number of mirrors in the optical path. It then will support two pairs of counterpropagating beams, one pair right and one pair left circularly polarized *(as referenced to a fixed point in one arm of the laser)*. The differential phase shifts for the *RCP* and *LCP* pairs are equal and opposite.

C. Longitudinal Kerr Effect

We have carried out a Jones matrix analysis of longitudinal $M-O$ Kerr effect mirrors in a ring laser gyro system. This analysis indicates that for a three (or other odd number) mirror laser the

differential phase shift would depend on Q^2 rather than Q so that such a case would not be useful. However, in a four (or other even) mirror system there are differential phase shifts linearly dependent on Q. The approximate normal modes of such a system are orthogonal linearly polarized beams of the form

$$E_A = E_p + E_s, \qquad E_D = E_p - E_s$$

where the E_i is the electric vector. The longitudinal analysis below is therefore cast in terms of E_A and E_D. The Fresnel coefficients are then

$$\begin{bmatrix} R_{AA} & R_{AD} \\ R_{DA} & R_{DD} \end{bmatrix} = \frac{1}{2} \begin{bmatrix} (R_{pp} + R_{ss} + R_{ps} + R_{sp}) & (R_{pp} - R_{ss} - R_{ps} + R_{sp}) \\ (R_{pp} - R_{ss} + R_{ps} - R_{sp}) & (R_{pp} + R_{ss} - R_{ps} - R_{sp}) \end{bmatrix}. \tag{20}$$

Again, since $R_{ss} \simeq -R_{pp}$ and $R_{ps} \simeq -R_{sp}$, we get $|R_{AD}|, |R_{DA}| >> |R_{AA}|, |R_{DD}|$ and hence the polarization essentially switches $A \rightarrow D$ and $D \rightarrow A$ at each mirror.

1) Differential Phase Shift

$$\Delta\Phi_L = Arg\{R_{AD}\} - Arg\{R_{DA}\} \tag{21}$$

2) Reflectivity

$$\begin{aligned} |R_{AD}(0)|^2 &= |R_{DA}(0)|^2 \\ &= \frac{1}{4}|R_{pp}(0) - R_{ss}(0)|^2 \end{aligned} \tag{22}$$

3) Differential Reflectivity

$$\Delta R_L = (|R_{AD}|^2 - |R_{DA}|^2)/|R_{AD}(0)|^2 \tag{23}$$

4) Mode Mixing

$$\epsilon_{LA} = |R_{AA}/R_{DA}|. \tag{24a}$$

$$\epsilon_{LD} = |R_{DD}/R_{AD}|. \tag{24b}$$

The computer program is set up to actually carry out the calculations sketched above, keeping track of which mode (transverse, polar or longitudinal) is being used and hence selecting the correct equations to evaluate the desired quantities.

III. THE COMPUTER MODEL

The basic calculation which the computer model must make is to determine the 4 × 4 scattering matrix (S) for a multilayer magnetic-dielectric structure of the type shown in Fig. 1. As shown by Eq. (10) in the last chapter, this means one must evaluate the scattering matrices (S^k) for each interface-layer and perform the indicated matrix mutliplication. Based on (S) one can calculate R_{pp}, R_{ps}, R_{sp} and R_{ss} for the entire $M-O$ structure. These are sufficient to evaluate the differential phase shift, reflectivity, differential reflectivity and mode mixing, as well as the figure of merit, for any of the three $M-O$ modes which might be used in a ring laser gyro magneto-optical mirror.

The simplest form of a flow diagram representing the computer model set up in this report is shown in Fig. 2. This carries out the calculation outlined in the last paragraph and serves to introduce the subroutines MOIN, MODIEL, MOMPL, MOMT, MOOUT and MOPLOT. We adopted a philosophy of breaking the main program MOFILM into a series of subroutines with the knowledge that *different* users would have different computer facilities which might require changes in MOIN, MOOUT and MOPLOT. Also users might wish to modify the calculation to suit their own special application. Such changes are simplified by the modular approach used here.

The actual structure of MOFILM is somewhat more complex than indicated in Fig. 2. This is due to two factors. The first is the need for the program to handle each of the three Kerr magneto-optical effects. For the transverse case MOFILM uses the subroutine MOMT when calculating the front and back surface scattering matrices for the magnetic layer. Both the polar and longitudinal cases, due to their formal similarity, are covered by MOMPL. Hence additional branching decision points are needed to distinguish which case is being handled and to direct the program to perform the proper calculation.

The second factor is related to the fact, that as shown in Fig. 2, MOFILM would make a single calculation of $\Delta\Phi$, R, ΔR, etc. for a fixed set of input constants. For design purposes, however, it is useful to see how these (or other) parameters vary as a function of changes in the input parameters.

As a result, we have set up MOFILM to permit easy variation of anyone of the following parameters: a) the thickness of the magnetic layer, b) the thickness of the dielectric layer immediately before or after the magnetic layer, or c) the angle of incidence. Hence, suitable DO loops are superimposed on the structure shown in Fig. 2.

Note that for calculations in which the thickness of one film is varied all but one of the scattering matrices remain the same. Hence when such a case is run the program stores the product scattering matrices for those parts of the multilayer structure before and after the varied layer. This saves considerable running time in determining the effect of such a thickness variation.

We now discuss the main program and the subroutines in greater detail. Program MOFILM carries out the expanded version of Fig. 2 outlined above. Consistent with the ideas given earlier, the MOFILM main program is mainly a logical skeleton which directs the use of suitable subroutines to make the actual calculations. Because of its heavily logical nature, particular care should be exercised in making alternations in the main program. To aid in any such alternations, the main program has extensive COMMENT statements to clearly define the functions being carried out. At NRL MOFILM is run on a PDP-11 computer in an interactive mode. Hence many of the TYPE statements in MOFILM are operator promptings and should be treated as additional COMMENT information. A print-out of MOFILM is given in the Appendix as are printouts of the subroutines used.

MOIN (NN) — This subroutine accepts all the needed input parameters and initializes the program, i.e., selects what $M-O$ mode is being used and what parameters (if any) are to be varied.

The inputs and their functions are:

$N(1)$	—	ambient index of refraction.
NF	—	number of layers in structure, including the substrate, $NF = 0$ used for program escape.
$M0$	—	layer number of magnetic layer.

LAMBDA — wavelength in microns.

(N, K) — complex index of refraction $n - ik$ of the magnetic layer.

(Q_1, Q_2) — complex magneto-optical coefficient $Q_1 - iQ_2$ of the magnetic layer.

N(I) — real index of the *I*th layers, $I = 1, \ldots, NF$.

D(I) — thickness of *I*th layer in microns, $I = 1, \ldots, NF$. It is not necessary to insert thickness values for those layers which have a phase thickness of $\pi/2$ (i.e., $d = \lambda/4n \cos\theta$) since the program automatically assumes this. If other fixed thicknesses for various layers are desired, they can be entered.

THETA — initial angle of incidence, in degrees.

NTH — number of THETA values.

DTH — increment in THETA, degrees.

L — layer number of layer whose thickness is to be varied.

MTH — number of L-layer thicknesses.

DELMD — increment in L-layer thickness, microns

NOUT — output control

NOUT = 1 printed output

NOUT = 2 graphic output

NOUT = 3 both outputs

NOUT = 0 return to beginning of input

NLTP — controls which Kerr effect used

NLTP = −1 longitudinal

NLTP = 0 transverse

NLTP = 1 polar

NN — input control

NN = 0 initial input

NN = 1 additional polarizations

This subroutine also calculates the sine and cosine of the angle of incidence in each layer including the complex values in the magnetic layer.

MODIEL(J,DJ) — This subroutine calculates the dielectric-dielectric scattering matrix shown in Eq. (9) and reports it back to the main program.

J — interface number

DJ — thickness of Jth layer = $D(J)$, in microns.

MOMPL(M, NPL, MD, D) — This subroutine calculates the magnetic-dielectric scattering matrix for the longitudinal or polar case and reports it back to the main program. The equations used are shown in Tables I, II, III and V.

NPL — control variable

NPL = +1 polar

NPL = -1 logitudinal

M — magnetic layer number

MD — specifies front or back surface calculation

$MD = M-1$ front surface

$MD = M + 1$ back surface

D — thickness of second layer, microns.

MOMT (M, MD, D) — This subroutine calculates the magnetic-dielectric scattering matrix for the transverse case and reports it back to the main program. The equations used are shown in Table I, IV and VI.

M, MD, D — defined in MOMPL earlier

MOOUT (NENT, IN) — This subroutine calculates the multilayer Fresnel coefficients R_{pp}, R_{ss}, R_{ps} and R_{sp} as well as $\Delta\Phi_l$, R_l, ΔR_l, ϵ_l and the figure of merit based on the scattering matrix for the full

stack. MOOUT also outputs the desired data with the necessary labels in either a printed or a plotted format or both. To perform plotting MOOUT calls on MOPLOT. MOOUT makes use of the equations in Table VII as well as Eqs. (10) to (12), Eqs. (13) to (17) or Eqs. (18)-(22) as appropriate.

NENT — controls entry point in MOOUT

IN — keeps track of sign of Q.

MOPLOT (NLTP, MTH, NO, LM1, DELMD) — This subroutine produces suitable plots of the variation of output parameters such as differential phase shift, total reflectivity, differential reflectivity, mode mixing and figure of merit as a function of the thickness of the magnetic layer or of nearby "tuning" layers. It will also plot output as a function of the initial angle of incidence. Since this subroutine makes use of local plotting subroutines which often vary from one facility to another, it will probably require modifications or complete revision in order to operate at another facility. The subroutine listing is given in the Appendix, however, to illustrate the functions needed.

N0 — *control variable*

N0 = 2 angle varied

N0 = 1 thickness varied

NLTP, MTH, DELMD — defined earlier in MOIN

LM1 — control variable for graph captioning

LM1 = 0 layer just before magnetic layer varied

LM1 = 1 magnetic layer varied

LM1 = 3 layer just after magnetic layer varied

Certain mathematical subroutines used in MOFILM are contained in our local matrix library and may not be available at other facilities. We define their functions here. It may be desireable to substitute local variants for these.

CSCLA (SD, X, 4, 4, 0) — sets each element in the complex 4 × 4 matrix SD equal to the complex number X.

CDCLA (SD, X, 4, 0) — sets each diagonal element in complex 4 × 4 matrix SD equal to the complex number X.

CMCPY (R, S, 4, 4, 0) — carries out the functions $S_{ij} = R_{ij}$ for each element of the 4 × 4 complex matrices S and R i.e., it copies R into S.

CMPRD (R, S, T, 4, 4, 0, 0, 4) — carries out the matrix product $T = R \times S$ for the 4 × 4 complex matrices R, S and T.

This completes our discussion of the details of program MOFILM. The printout of the main programs and each of the subroutines MOIN, MODIEL, MOMPL, MOMT, MOOUT and MOPLOT are located in the Appendix. The above discussion in conjunction with the COMMENT statements and some of the TYPE statements in MOFILM and its subroutines should make the operation of the program fairly straightforward. However, this chapter should be read carefully in conjunction with the Appendix to avoid the common GIGO syndrome.

IV. TYPICAL MULTILAYER CALCULATIONS

To illustrate the capabilities of program MOFILM, in this chapter we carry out a number of calculations of the magneto-optical and optical characteristics of several magnetic-dielectric multilayer thin film structures. In particular, typical structures of the type which might be used as magnetic bias mirrors in ring laser gyros are emphasized. The results of the calculations show the usefulness of the program as a design tool for comparing various mirror designs or optimizing the parameters of a given design.

Typical structures which might be used for an RLG magnetic mirror are:

A. An opaque magnetic metal film overcoated with a multilayer dielectric (MLD) stack.

B. A transparent non-metallic magnetic film, such as a garnet, on top of an MLD stack.

C. A partially transparent (very thin) magnetic metal film on top of an MLD stack.

We also discuss how the figure of merit FM, which we define as

$$FM = \Delta\Phi/(1 - \text{Reflectivity}) \tag{25}$$

is affected by the design parameters.

In order to make things definite we assume that the dielectric stack is made up of layers of SiO_2 with a real index of refraction $n(SiO_2) = 1.457$ and ZnS with $n(ZnS) = 2.355$. We ignore the small changes in $n(SiO_2)$ and $n(ZnS)$ between $\lambda = 0.63\ \mu m$ and $1.15\ \mu m$, since the results are rather insensitive to these changes, especially if the layers have fixed phase thicknesses as is true for much of the MLD stack. We also take $\theta_{initial} = 30°$ and use the values of n, k, Q_1, and Q_2 in Table VIII for the magnetic layer under study. We now discuss the above cases in some detail.

Table VIII. Parameters of Magnetic Materials Used in Multilayer Mirror Calculations

Material	λ (μm)	n	k	Q_1	Q_2	Ref.
Fe	1.15	3.7	5.1	0.053	−0.036	17
MnBi	0.63	2.7	3.0	−0.089	0.073	15
MG3	0.63	2.2	0.005	0.0038	0.0(?)	16

MG 3 = $(Gd,Pr,Bi)_3$ $(Fe,Ga)_5$ O_{12} with θ_F = 25,200 deg/cm and $\alpha = 4\pi k/\lambda$ estimated to be 1000 cm^{-1}.

A. MLD stack on top of an opaque magnetic film

The general form we take for this mirror is $n(L - H) - M$ where L is a low index and H, a high index dielectric and M is the opaque magnetic substrate. All the layers except that adjacent to M are taken to have a phase thickness $\phi_i = (2\pi n_i d_i \cos\theta_i/\lambda) = \pi/2$ in order to maximize the MLD reflectivity for the given $\theta_{initial}$. We have examined cases with an odd number of dielectric layers and the results are qualitatively similar to those shown here. In this design, as the reflectivity is improved by adding more layers, less and less light reaches the magnetic layer so that the differential phase shift $\Delta\Phi$ of the total structure is decreased.

Transverse case — Note that $\Delta\Phi$ depends on (a) the relative amplitudes of the electric vector for the total light reflected from the mirror and that part of the electric vector of the light reflected from the magnetic layer which reverses when the magnetization (and hence Q) reverses and b) the relative phase between these two vectors. This point has been discussed before [Report No. 2, Chap. III, Sect. A] [2].

Macek [10] pointed out how one can tune the relative phase by adjusting the thickness of the dielectric "tuning" layer next to the magnetic layer. (We recall that only a p-polarized beam has an $M-O$ effect for the transverse case so all results refer to the counterpropagating p-polarized beams.) To illustrate this effect we assume that the mirror is $6(L - H) -$ Fe with the 1.15 μm Fe parameters in Table VIII.

The dependence of $\Delta\Phi$, the p reflectivity R, and ΔR on the tuning layer thickness d_{M-1} is shown in Figs. 3-5. (The notation $/1K$ on a scale means the actual unit is 10^{-3} times that shown, for $/E5$ it is 10^{-5} times, etc.) Note that there is a "resonant" behavior in all these quantities when $d_{M-1} \simeq 0.10\ \mu$m. Near this d_{M-1} value the first few dielectric layers adjacent to the magnetic layer act like an impedance transformer to couple the light efficiently into the lossy magnetic film. This means that the non-Q dependent electric vector of the multiply-reflected beam from the magnetic layer adds out of phase with that from the adjacent layers giving rise to the dip in R. The Q-dependent electric vector of the multiply-reflected magnetic-layer beam has a different phase associated with it and hence gives rise to the enhancement and rapid variation of $\Delta\Phi$ and ΔR for d_{M-1} near 0.1 μm. Note that $\Delta\Phi$ is maximized at nearly the same d_{M-1} value for which ΔR is zero as anticipated by the simple analysis [Report No. 2, pp. 9-11] [2] which neglects multiple reflection effects. The variation of the figure of merit with d_{M-1} is shown in Fig. 6.

By examining such results for mirrors with different numbers of layers in the MLD stack one can find how $(\Delta\Phi)_{max}$ varies with the corresponding total mirror loss $(1 - R)$. The results are shown in Fig. 7 where $(\Delta\Phi)_{max}$ is clearly proportional to the mirror loss. Thus $(\Delta\Phi)_{max}/(1 - R)$ is a constant for a given magnetic material (and θ, n_L, n_H), independent of the details of the MLD design and hence serves as a useful figure of merit to characterize the magneto-optical materials used as opaque substrates. This type of analysis was used in Fig. 9 of Report No. 2 [2].

Polar case — The same type of calculations presented for the transverse case were repeated for the polar case using the same mirror. In addition, the mode mixing ϵ_R [see Eq. (19a)] was calculated. Remember that in the polar case $\Delta\Phi$ and ΔR refer to the difference between incoming RCP and LCP beams. The behavior of R is so similar to Fig. 4 that it is not plotted. The other results are shown in Figs. 8-11. The qualitative features of $\Delta\Phi$ and ΔR as a function of the d_{M-1} also resemble the transverse case. However, we wish to draw attention to the fact that one obtains a much larger differential phase shift (and ΔR) in the polar case even for the same magnetic metal, (cf., Figs. 3 and 8

and Figs. 5 and 9). There is a corresponding increase in *FM*. The mode mixing ϵ_R in Fig. 11 is an optical (not a magneto-optical) effect. For the case shown here the amplitude of the "wrong" electric vector is 2.5% that of the correct one at Φ_{max}.

Finally, to illustrate what can be accomplished with an opaque polar Kerr mirror based on MnBi we show Figs. 12 and 13. Note that because MnBi has its magnetization normal to the plane of the film (if properly constructed), it is well suited for polar Kerr use. Actually Fe, which was shown in the previous example, is *not* suitable for use in the polar mode since the shape anisotropy causes its magnetization to lie in the plane of the film.

B. "Transparent" magnetic film on top of an MLD stack

In this case we take the general form of the mirror to be $M - n(L - H)$. Also we take $\phi_i = \pi/2$ for all the dielectric layers so as to maximize the reflectivity. In contrast to case A, in this design all of the light impinging on the mirror reaches the magnetic layer. As a result, $\Delta\Phi$ stays constant as one adds more layers to the MLD stack. By the designation "transparent," we mean that $k_M << n_M$ for the magnetic film. In general, there is some optical loss in this film and, especially at 0.63 μm, this may be the limiting factor in the performance of the mirror.

The idea of using combinations of "transparent" magnetic layers and MLD stacks as biasing elements in ring laser gyros has been advanced earlier [5,12]. Here we merely show the capabilities of MOFILM for handing such designs and illustrate some of the general features of their behavior. For the magnetic layer we take Bi-doped garnet MG3 shown in Table VIII for 0.63 μm and, in contrast to case A, we vary the thickness of this layer to properly phase match the Kerr reflections at its front and back surfaces. Since it is likely that magnetic garnets will be grown by liquid phase epitaxy on a substrate of GGG (gadolinium gallium garnet), we assume that the incoming light beam is traveling in a medium having the real index of refraction of GGG, viz $n(GGG) = 1.95$.

Transverse case — To allow easy comparison with case A the mirror stack is taken to be MG3 − 6(L − *H*). Results for $\Delta\Phi$, R, ΔR and FM are shown in Figs. 14-17, respectively. In contrast to case A, these quantities are slowly varying functions of the thickness varied (d_M in this case). The differential phase shift for *p*-polarized light is maximized when the effective optical thickness is nearly $\lambda/4$. The slow decrease in R with increasing d_M is due to the non-trivial value of k (corresponding to an optical absorption coefficient $\alpha = 1000\ \text{cm}^{-1}$). At $\lambda = 1.15\ \mu\text{m}$, magneto-optic garnets exist with k small enough to be negligible. The differential reflectivity ΔR is very small for the case shown here with $Q_2 = 0$. If one allows Q_2 to be of the same order of magnitude as Q_1, then ΔR increases by a large amount (see Fig. 18). In fact, to a good approximation for magnetic materials with $k << n$, we find $\Delta\Phi$ is proportional to Q_1 while ΔR is proportional to Q_2. Furthermore, ΔR peaks at the same value of d_M as does $\Delta\Phi$ if Q_2 is significant.

Although we plot *FM* vs d_M in Fig. 17, we wish to emphasize that $\Delta\Phi/(1 - R)$ is not such a good figure of merit in the case where one has a "transparent" magnetic overlayer on a MLD stack. Since $\Delta\Phi$ remains constant when more layers are added to the MLD while the reflectivity increases, $\Delta\Phi/(1 - R)$ is a function of the number of layers. Nevertheless, one sees that the phase shift per unit loss is much larger for the garnet mirror shown here than for the Fe-based mirror in case A. (If we were to compare both mirrors at 0.63 μm, the difference would be even more marked.) If k is large enough (as it is at 0.63 μm), then $\Delta\Phi/(1 - R) = FM$ does acquire a limiting value when more bilayers are added to the stack and its usefulness as a true figure of merit is restored.

Polar case — The results of calculations for a similar 0.63 μm mirror operating in the polar mode are given in Figs. 19-21. Again all the calculated quantities are slowly varying functions of d_M. Perhaps the most surprising result is the fact that, in contrast to case A, $(\Delta\Phi)_{max}$ is about the same size for both the polar and transverse Kerr effects (cf., Figs. 14 and 19). We point out that in the polar and longitudinal Kerr modes MOFILM takes into account the Faraday rotation in the magnetic film.

C. Very thin absorbing magnetic film on an MLD stack

This case is an extension of case B to the region where k is comparable to n. This allows one to investigate the effect of Faraday rotation and the Kerr reflection from the back surface of a metallic magnetic film. The mirror structure is Fe $-$ $6(L - H)$ and the thickness of the magnetic layer is varried. The results for this case are given for a transverse mirror in Figs. 22-25. This is merely illustrative of what can be accomplished with very thin magnetic films.

D. Comparisons and comments on the preceeding cases

A typical 40 cm perimeter ring laser gyro requires a bias frequency of 50 kHz or more to prevent lock-in and obtain a constant scale factor. This implies that the differential phase shift between the similar counterpropagating beams must be $\geqslant$ 0.4 mrad (0.023 deg). Typically one requires optical losses $\leqslant$ 5% at 1.15 μm and $\leqslant$ 1-2% at 0.63 μm. The required characteristics of a magnetic-dielectric mirror structure for RLG use are thus:

1) $\Delta\Phi \geqslant 0.4$ mrad

2) $FM \geqslant \begin{cases} 8 \text{ mrad} & 1.15\ \mu\text{m} \\ 20\text{–}40 \text{ mrad} & 0.63\ \mu\text{m} \end{cases}$

3) No insuperable manufacturing problems.

Figure of merit values for a number of mirror designs operating in either the transverse or the polar mode at both 0.63 μm and 1.15 μm are given in Table IX. This table is taken from the recent review [3] of applications of magneto-optics in ring laser gyroscopes.

As yet no magnetic alloy suitable for use in a transverse Kerr $M-O$ mirror has been found whose magneto-optical performance significantly exceeds that of pure Fe [3,13]. Table IX indicates that such a Fe-based mirror is barely adequate at 1.15 μm while it would not satisfy requirement 2) at 0.63 μm. On the other hand, MnBi operating in a polar mode easily meets these requirements at 0.63 μm. Although we do not have index and magneto-optical coefficient data on MnBi at 1.15 μm, it is likely to

Table IX. Magneto-optical Figure of Merit for Magnetic Metal and Garnet Based Mirrors

Mirror Design	Mode	$\Delta\Phi$/(opt. loss)	λ (μm)
MLD on Fe	Trans.	10	1.15
MG4 on MLD	Trans.	>400	1.15
MG4 on MLD	Polar	>300	1.15
MLD on Fe	Trans.	6	0.63
MLD on MnBi	Polar	>85	0.63
MG3 on MLD	Trans.	230	0.63
MG3 on MLD	Polar	210	0.63

MG4, (n = 2.19, k = 1×10^{-4}, θ_F = 1700 deg/cm) MG3, see Table VIII.

work well at that wavelength also. The principal problem with MnBi-based RLG mirrors would seem to be the manufacture of films which actually meet the calculated performance. This is clear from a literature review of the optical and magneto-optical properties as well as the physical structure of MnBi thin films [14,15].

One other problem with the metallic-based mirrors is the fact that $\Delta\Phi$ is such a strongly varying function of d_{M-1}. To achieve $\Delta R \simeq 0$ and $\Delta\Phi \simeq (\Delta\Phi)_{max}$ means that d_{M-1} must be held to tolerances of roughly 50-100 Å if one operates in the neighborhood of the "resonance." One can try to get around this problem by operating away from the "resonance" with a smaller number of layers in the MLD stack to increase $\Delta\Phi$. Such an approach allows Fe at 1.15 μm to remain marginally useful but does get around the thickness tolerance problem for MnBi-based mirrors (see Figs. 19 and 21).

The garnet-based mirrors do not have this problem because of their slow variation of $\Delta\Phi$ with d_M. Furthermore, their figure of merit values as indicated in Table IX are more than adequate. Their principal difficulties are attaining an adequate $\Delta\Phi$ and the fact that the ΔR peak occurs at the same d_M for

which $\Delta\Phi$ is maximized. Although there exist actual garnets (for transverse Kerr mode operation) which have acceptable $\Delta\Phi$ values, there is little or nothing known about their Q_2 values and the consequent ΔR's. For the garnet-based transverse Kerr mirrors of Table IX the $\Delta\Phi_{max}$ values are 0.8 and 2.6 mrad at 1.15 and 0.63 μm, respectively and hence are adequate.

The above considerations indicate that garnet-based mirrors represent a good approach to magnetic biasing for ring laser gyros. However, the good performance of MnBi in the polar Kerr mode at 0.63 μm means that it is a viable alternative for constructing such mirrors. For the magnetic garnets it is desirable to develop materials with the largest Faraday rotation possible at the wavelength of interest while keeping k and Q_2 as small as possible. Previous materials characterization work [16] has indicated that variants of yttrium iron garnet (*YIG*, $Y_3Fe_5O_{12}$) which contain significant amounts of Bi and Pr plus *Yb* and/or *Gd* as dopants have achieved the largest Faraday rotations consistent with low k. It is important to characterize the Q_2 values of such garnets but no data on this exists to our knowledge.

APPENDIX

In this Appendix we give the computer listing of program MOFILM as well as those of the subroutines MOIN, MODIEL, MOMPL, MOMT, MOOUT and MOPLOT. These routines are supported by certain matrix routines which are not listed here but whose functions are defined in Chapter III. Likewise MOPLOT is supported by a number of subroutines which perform scaling, labelling, tick mark, etc. functions involved in making the actual plots of the computer calculations. It is anticipated that local versions of MOPLOT will probably be written to suit local variations in handling plots.

A study of these listings together with their functional descriptions given in Chapter III and the COMMENTS and TYPE statements imbedded in the listings should give the reader a fairly detailed understanding of the overall program and permit him to make alternations which may better suit his own situation. In the final analysis all of the useful optical and magneto-optical information about a given magnetic-dielectric multilayer structure is contained in the complex components of the scattering matrix(S) and hence any useful parameter describing the behavior of the structure can be obtained from (S). This includes the transmission and Faraday rotation properties which are not discussed in detail here but which are given in Table VII.

The various input parameters and the calling parameters for the various subroutines are given in Chapter III. Most of the transfer of information among the subroutines and between the subroutines and the main program are carried out via COMMON statements.

```
C     ------------------------------------------------------------------
C
C       PROGRAM MOFILM
C
C       PURPOSE
C          CALCULATES MAGNETO-OPTICAL PROPERTIES OF MULTILAYER
C          THIN FILM SYSTEMS
C
C       SUBROUTINES REQUIRED
C          MOIN(NN)
C          MOOUT(NENT,IN)
C          MODIEL(K,DK)
C          MOMPL(M,NPL,MD,0)
C          MOMT(M,MD,0)
C          MOPLOT(N,M,NO,L,DELX)
C          THE CALLING PARAMETERS,EXCEPT IN MOPLOT, ARE
C               NN,NENT - ENTRY POINTS
C               IN - BRANCHING CONTROL, RELATED TO SIGN OF Q
C               K,M,MD - LAYER NOS.
C               DK,D - LAYER THICKNESSES
C               NPL - POLARIZATION
C          FOR MOPLOT, THE PARAMETERS ARE
C               N -POLARIZATION
C               M - NO. OF VALUES INCREMENTED VARIABLE
C               NO - VARIABLE INCREMENTED (D OR THETA)
C               L - LAYER VARIED
C               DELX - INCREMENT
C
C       LIBRARY ROUTINES REQUIRED
C          COMPLEX MATRIX ROUTINES FROM DEC MATH LIBRARY
C               CSCLA,CDCLA,CMFRD,CMCPY
C          PLOTTING ROUTINES FROM TEKTRONIX
C
C       LOCAL ROUTINES
C          SCLRND, SIZE, PAUSE ARE USED IN MOPLOT
C          SEE EXPLANATION THERE
C
C       INPUT REQUIRED
C          REFRACTIVE INDICES OF ALL LAYERS
C          COMPLEX REFRACTIVE INDEX AND COMPLEX MAGNETO OPTIC
C            COEFFICIENT FOR MAGNETIC LAYER
C
C     ------------------------------------------------------------------
      PROGRAM MOFILM
      IMPLICIT COMPLEX (R)
      COMPLEX SP(4,4),D1(4,4),S(4,4),STM,CTM,NM,ZI,D1T(4,4),SD(4,4),D,I
     1,D2T(4,4)
      REAL LAMBDA,N(30),RRLP2,RPPP2,RPPN2,RPPT2
      REAL*8 DDENT(5),POL(3)
      DIMENSION RPP(101),RPS(101),RSP(101),RSS(101),RRLP2(101),
     1DPHIP(101),EPS(101),DREFL(101),RPPT2(101),DPHIT(101),DELRP(101
     2,RPPP(101),RPPN(101),D(30),ST(30),CT(30),DT(3),DRAY(12),DD(4)
     3COMMON /D1/LAMBDA,N,D,NM,PLTF,DI,CT,ST,CTM,STM/SOUT/S,DD,NXD
```

```
      1/A=RPLT/RRLP2,DPHIP,EPS,DREFL,XO/ID/DDENT,DT,JPLOT
      2/INOUT/NFO,MO,LO,NTH,DTHO,THETAD,MTH,DELMD,NOUT,NLTF
      EQUIVALENCE (RPP(1),RPPF(1)),(RPS(1),RPPN(1)),(RRLP2(1),RPPT2(1)),
     1(DPHIP(1),DPHIT(1)),(EPS(1),DELRP(1))
      DATA POL/'LONG.','TRANSV.','POLAR'/
      DATA DRAY/'D(MA','G) (','MU)','D(M-','1) (','MU)',
     1'THET','A (D','EG)','D(M+','1) (','MU)'/
      NN=0
C     CALL FOR INPUT
100   CALL MOIN(NN)
25    CONTINUE
C     THE END?
      IF(NFO.EQ.0.) GO TO 100
      NFIL=4
      M=MO
      L=LO
      NF=NFO-1
      DM1=D(L)
      DM=D(M)
      NNFIL=0
      MNTH=MTH-NTH
      IF(MO .EQ. 0)M=NF+2
      LM1=1
      IF(M.GT.L) LM1=0
      IF(M.LT.L) LM1=3
      NPOL=NLTP+2
      DDENT(5)=POL(NPOL)
      THETA=THETAD*PI()/180.
      DTH=DTHO*PI()/180.
7     CONTINUE
      NINC=0
      IF(NN/2*2.NE.NN) NINC=1
      NN=NN-NINC
C     LOOP FOR THETA
      DO 2 ITH=1,NTH
      ST(1)=SIN(THETA)
      CT(1)=COS(THETA)
C     CALCULATE PROPAGATION ANGLES AND THICKNESSES
      DO 3 J=2,NF+1
      ST(J)=ST(1)*N(1)/N(J)
      CT(J)=SQRT(1.-ST(J)**2)
      IF(NN.EQ.2) GO TO 3
      D(J)=LAMBDA/(4.*N(J)*CT(J))
3     CONTINUE
      STM=ST(M-1)*N(M-1)/NM
      CTM=CSQRT(1.-STM**2)
      R1=(0.,0.)
      R2=(1.,0.)
      IF(ITH.NE.1) GO TO 5
      CF=1.
      IF(NINC.EQ.0) CF=LAMBDA/(N(L)*CT(L))
      DM1=DM1*CF
```

```
            DELMD=CF*DELMD
 5          D(1)=0.
            D(NF+1)=0.
            DM=D(M)
            D(L)=DM1
 C          PRINT OUT INPUT INFORMATION
            CALL MOOUT(1,0)
 C          LOOP FOR D(L)
            DO 10 JD=1,MTH
            DVAR=(JD-1)*DELMD
            IF(L .EQ. M) DM=D(M)+DVAR
            IF(L.NE.1.AND.L.NE.M) D(L)=DM1+DVAR
            DD(1)=DM
            DD(2)=D(L)
            DD(3)=180.*THETA/PI()
            DD(4)=D(L)
            IF (MNTH) 32,32,34
 32         J=ITH
            IF(ITH .EQ. 1) XO=DD(NXD)
            GO TO 35
 34         J=JD
            IF(JD .EQ. 1) XO=DD(NXD)
 C          INITIALIZE MATRICES
 35         CALL CSCLA(SO,R1,4,4,0)
            CALL CSCLA(SP,R1,4,4,0)
            CALL CSCLA(D1,R1,4,4,0)
            CALL CSCLA(S,R1,4,4,0)
            CALL CDCLA(SD,R2,4,0)
            CALL CDCLA(S,R2,4,0)
            CALL CDCLA(SP,R2,4,0)
            IF(NNFIL.EQ.0) CALL CSCLA(D1T,R1,4,4,0)
            IF(M .EQ. 2) GO TO 30
            JFMIN=2
            IF(NNFIL.EQ.1) JFMIN=M-1
            DO 4 JF=JFMIN,M-1
            IF(NNFIL.NE.1) GO TO 66
            CALL CMCPY(D1T,S,4,4,0)
 66         DJF=D(JF)
 C          CALCULATE FRONT STACK
            CALL MODIEL(JF,DJF)
            CALL CMPRO(S,D1,SD,4,4,0,0,4)
            CALL CMCPY(SD,S,4,4,0)
            IF(.NOT.(NFIL.EQ.4.AND.NNFIL.EQ.0.AND.JF.EQ.(M-2).AND.M.GE.4))
            1 GO TO 4
            CALL CMCPY(SD,D1T,4,4,0)
            NNFIL=1
 4          CONTINUE
 30         IF((M-NF) .EQ. 2) GO TO 102
 C          CHECK FOR POLARIZATION
            IF (NLTP) 101,301,101
 C          CALCULATE MAGNETIC LAYER FOR POLAR OR LONGITUDINAL POLARIZATIONS
 101        CALL MOMPL(M,NLTP,M-1,DM)
```

```
      CALL CMPRD(SD,D1,S,4,4,0,0,4)
      CALL CMCPY(S,SP,4,4,0)
      IF ((M-NF) .EQ. 1) GO TO 102
      CALL MOMPL(M,NLTP,M+1,D(M+1))
      CALL CMPRD(SP,D1,S,4,4,0,0,4)
      IF (.NOT.(NF .GT.M)) GO TO 102
      IF(NNFIL.NE.2) GO TO 105
      CALL CMCPY(S,SP,4,4,0)
      CALL CMPRD(SP,D2T,S,4,4,0,0,4)
      GO TO 102
105   CALL CMCPY(S,SP,4,4,0)
      CALL CSCLA(S,R1,4,4,0)
      CALL CSCLA(D1,R1,4,4,0)
      CALL CDCLA(S,R2,4,0)
      DO 40 JF=M+2,NF+1
      DJF=D(JF)
C     CALCULATE BACK STACK
      CALL MODIEL(JF,DJF)
      CALL CMPRD(S,D1,SD,4,4,0,0,4)
60    CALL CMCPY(SD,S,4,4,0)
40    CONTINUE
      CALL CMPRD(SP,SD,S,4,4,0,0,4)
      IF(.NOT.(NFIL.EQ.4.AND.NNFIL.EQ.0)) GO TO 102
      CALL CMCPY(SD,D2T,4,4,0)
      NNFIL=2
C     OUTPUT FOR POLAR AND LONGITUDINAL POLARIZATIONS
102   CALL MOOUT(2,IN)
      GO TO 10
301   IN=0
C     CALCULATE MAGNETIC LAYER FOR TRANSVERSE POLARIZATION
305   CALL MOMT(M,M-1,DM)
      CALL CMPRD(SD,D1,S,4,4,0,0,4)
      CALL CMCPY(S,SP,4,4,0)
      IF ((M-NF) .EQ. 1) GO TO 302
      CALL MOMT(M,M+1,D(M+1))
      CALL CMPRD(SP,D1,S,4,4,0,0,4)
      IF (.NOT.(NF .GT. M)) GO TO 302
      CALL CMCPY(SD,SP,4,4,0)
      IF(NNFIL.NE.2) GO TO 110
      CALL CMCPY(S,SD,4,4,0)
      CALL CMPRD(SD,D2T,S,4,4,0,0,4)
      GO TO 46
110   CALL CMCPY(S,D2T,4,4,0)
      CALL CSCLA(S,R1,4,4,0)
      CALL CSCLA(D1,R1,4,4,0)
      CALL CDCLA(S,R2,4,0)
      DO 45 JF=M+2,NF+1
      DJF=D(JF)
C     CALCULATE BACK STACK FOR TRANSVERSE POLARIZATION
      CALL MODIEL(JF,DJF)
      CALL CMPRD(S,D1,SD,4,4,0,0,4)
      CALL CMCPY(SD,S,4,4,0)
```

```
 45       CONTINUE
          CALL CMFRD(D2T,SD,S,4,4,0,0,4)
          IF(.NOT.(NFIL.EQ.4.AND.NNFIL.EQ.0)) GO TO 46
          CALL CMCPY(SD,D2T,4,4,0)
          NNFIL=2
 46       CALL CMCPY(SP,SD,4,4,0)
 C        OUTPUT FOR TRANSVERSE POLARIZATION
 302      CALL MOOUT(3,IN)
          IF(IN.EQ.1) GO TO 305
 10       CONTINUE
          D(L)=DM1
          IF(MNTH .LT. 0) GO TO 2
          IF(NOUT .EQ. 1) GO TO 21
 C        PLOT FOR VARIABLE D
          CALL MOPLOT(NLTP,MTH,1,LM1,DELMD)
 21       CALL CLEAR
 2        THETA=THETA+DTH
          IF (MNTH .GT. 0) GO TO 52
          IF(NOUT .EQ. 1) GO TO 51
 C        PLOT FOR VARIABLE THETA
          CALL MOPLOT(NLTP,NTH,2,0,DTHO)
 51       CALL CLEAR
 52       NN=1
 C        MORE INPUT?
          GO TO 150
 100      STOP
          END



          SUBROUTINE MOIN(NN)
 C        THIS SUBROUTINE ACCEPTS INPUT
          COMPLEX Q,NM
          BYTE YAL
          REAL LAMBDA,N
          REAL*8 DDENT(5)
          DIMENSION N(30),D(30),DT(3),I(30)
          COMMON /DI/LAMBDA,N,Q,D,NM/ID/DDENT,DT,JPLOT
          COMMON /INOUT/NFO,MO,LO,NTH,DTHO,THETAD,MTH,DELMD,
          INOUT,NLTP
          IF(NN.EQ.1) GO TO 15
 C        REENTER DATA? OR JUST CHANGE OUTPUT?
 150      CALL CLEAR
          TYPE *,' ALL INPUT, EXCEPT FOR ALPHANUMERIC, IS ACCEPTED'
          TYPE *,' BY LIST DIRECTED STATEMENTS'
          TYPE *,' TO ENTER RUN I.D., TYPE Y, IF NOT, (CR)'
          ACCEPT 152,YAL
 152      FORMAT(1A1)
          IF(YAL .NE. ' ') GO TO 155
          TYPE *,' TYPE RUN IDENTIFICATION (UP TO 32 CHARACTERS)'
          ACCEPT 40,DDENT
```

```
42      FORMAT(5A8)
155     TYPE *,' THE NUMBER OF LAYERS (NF) IN THE GENERAL CONFIGURATION'
        TYPE *,' IS ARRANGED AS FOLLOWS'
        TYPE *,'       AMBIENT(1)'
        TYPE *,'       DIELECTRIC LAYERS'
        TYPE *,'       MAGNETIC LAYERS'
        TYPE *,'       DIELECTRIC LAYERS'
        TYPE *,'       AMBIENT(NF)'
        TYPE *,' ONE OR MORE OF THESE MAY BE OMITTED, EXCEPT THAT'
        TYPE *,' THE TERMINATING LAYERS MUST BE AMBIENT, I.E., OPAQUE'
        TYPE *,' OR TRANSPARENT (NO LIGHT SCATTERED BACK INTO SYSTEM).'
        TYPE *,' NF = NO. OF FILMS (NF = 0 TO ESCAPE)'
        TYPE *,' M = MAGNETIC FILM NUMBER (M = 0 IF NO MAGNETIC FILM)'
        TYPE *,' LAMBDA  = WAVELENGTH (MICRONS)'
        TYPE *,' NM = COMPLEX REFRACTIVE INDEX OF MAGNETIC LAYER'
        TYPE *,' Q = COMPLEX M-O COEFFICIENT'
        TYPE *,' TYPE NF, M, LAMBDA, (N,K), (Q1,Q2)'
        ACCEPT *, NFO,MO,LAMBDA,NM,Q
        IF(NFO.EQ.0.) RETURN
22      TYPE *,' N(I) = ITH REFRACTIVE INDEX (NOT ITH LAYER)'
        TYPE *,' NN = NO. OF LAYERS HAVING THAT INDEX'
        TYPE *,' I(1),..,I(NN) = LAYERS HAVING THAT INDEX'
        TYPE *,' TYPE NN,N(I),I(1),...,I(NN)'
        TYPE *,' (TO ESCAPE LOOP,TYPE /(CR))'
        N(MO)=REAL(NM)
12      ACCEPT*,IJ,REF,(I(J),J=1,IJ)
        IF(IJ.EQ.0) GO TO 11
        DO 5 J=1,IJ
5       N(I(J))=REF
        IJ=0
        GO TO 12
11      CONTINUE
        IF(NN.EQ.0) GO TO 10
        TYPE *,' IF YOU WISH TO KEEP PRESENT VALUES OF THICKNESSES'
        TYPE *,' TYPE Y'
        ACCEPT 152,YAL
        IF(YAL.EQ.'Y') GO TO 20
10      CALL CLEAR
        TYPE *,' THE PHASE THICKNESS OF A LAYER IS DEFINED AS'
        TYPE *,' DO(I) = LAMBDA/N(I)*COS(THETA(I))'
        TYPE *,' (THETA(I) IS THE PROPAGATION DIRECTION)'
        TYPE *,' THE THICKNESS OF EACH LAYER IS CALCULATED AS D(I)*A
        TYPE *,' IF YOU WISH TO CHANGE THE D'S, TYPE Y'
        TYPE *,' (NO ENTRY REQUIRED FOR VARIABLE LAYER AT THIS TIME)
        NN1=0
C       D'S ENTERED IN PHASE THICKNESSES
        ACCEPT 152,YAL
        IF(YAL.NE.'Y') GO TO 20
40      TYPE *,  D(I) =THICKNESS OF ITH LAYER (MICRONS)'
        TYPE *,' ND = NO. OF LAYERS HAVING THAT THICKNESS
        TYPE *,' I(1),...I(ND) = LAYERS HAVING THAT THICKNESS
        TYPE *,' TYPE ND,D(I),I(1),...I(ND) (CR) FOR EACH D(I)
```

```
      TYPE *,' (D''S NOT REQUIRED FOR AMBIENT OR VARIABLE LAYERS)'
      TYPE *,' (TO ESCAPE LOOP, TYPE /(CR))'
   32 ACCEPT *,IJ,DTEMP,(I(J),J=1,IJ)
      IF (IJ.EQ.0) GO TO 20
      DO 30, J=1,IJ
   30 D(I(J))=DTEMP
      IJ=0
      NN1=2
C     D'S ENTERED IN MICRONS
      GO TO 32
   20 CALL CLEAR
      TYPE *,' NTH = NO. OF VALUES OF THETA'
      TYPE *,' THETA = INITIAL VALUE OF ANGLE OF INCIDENCE'
      TYPE *,' DTH = INCREMENTAL VALUE'
      TYPE *,' L=LAYER TO BE VARIED IN THICKNESS (M+1, M, OR M-1)'
      TYPE *,' MTH = NO. OF VALUES OF L LAYER THICKNESSES'
      TYPE *,' TYPE NTH,THETA,DTH,L,MTH'
      ACCEPT *,NTH,THETA0,DTH0,L0,MTH
      TYPE *,' LAYER L IS USUALLY VARIED BY 1/2 PHASE THICKNESS'
      TYPE *,'    DL0 = INITIAL THICKNESS OF L (USUALLY 0)'
      TYPE *,'    DL1 = FINAL THICKNESS OF L'
      TYPE *,'    NINC = 0 FOR DL0, DL1 IN PHASE THICKNESSES'
      TYPE *,'           1  "   "    "   " MICRONS'
      TYPE *,' TYPE NINC,DL0,DL1'
      ACCEPT *,NINC,DL0,DL1
   15 TYPE *,' NOUT = 1 FOR PRINTED OUTPUT'
      TYPE *,'        2 FOR GRAPHIC OUTPUT'
      TYPE *,'        3 FOR BOTH'
      TYPE *,'        0 TO GO TO BEGINNING OF INPUT'
      TYPE *,' NLTP = -1 FOR LONGITUDINAL CASE'
      TYPE *,'         0 FOR TRANSVERSE CASE'
      TYPE *,'         1 FOR POLAR CASE'
      TYPE *,' JPLOT = 1 TO SUPPRESS DATE ON GRAPH CAPTION'
      TYPE *,'         0 OTHERWISE'
      TYPE *,' TYPE NOUT,NLTP,JPLOT'
      TYPE *,' TYPE 0/(CR) TO RETURN TO BEGINNING OF INPUT'
      ACCEPT *,NOUT,NLTP,JPLOT
      D(L0)=DL0
      DELMD=(DL1-DL0)/(MTH-1)
      IF (NOUT .EQ. 0) GO TO 150
      NN=NN1-NINC
      RETURN
      END
```

```
      SUBROUTINE MODIEL(K,DK)
      DIMENSION D1(4,4),N(30),CT(30)
      IMPLICIT REAL (N)
      REAL LAMBDA
      COMPLEX CX,PROP,PROPN,D1,R1,NM,Q,CTM,STM
      COMMON /DI/LAMBDA,N,Q,D(30),NM/PLTF/D1,CT,ST(30),CTM,STM
      NC12=N(K-1)*CT(K)
      NC11=N(K-1)*CT(K-1)
      NC22=N(K)*CT(K)
      NC21=N(K)*CT(K-1)
      PHI=2.*PI()*(DK*N(K)*CT(K)/LAMBDA)
      CX=(0.,1.)*PHI
      PROP=CEXP(CX)
      PROPN=CEXP(-CX)
      RPP=(NC21-NC12)/(NC21+NC12)
      RSS=(NC11-NC22)/(NC11+NC22)
      TPP=N(K-1)*(1.+RPP)/N(K)
      TSS=1.+RSS
      R1=(0.,0.)
      CALL CSCLA(D1,R1,4,4,0)
      D1(1,1)=PROP/TPP
      D1(1,3)=PROPN*RPP/TPP
      D1(2,2)=PROP/TSS
      D1(2,4)=PROPN*RSS/TSS
      D1(3,1)=PROP*RPP/TPP
      D1(3,3)=PROPN/TPP
      D1(4,2)=PROP*RSS/TSS
      D1(4,4)=PROPN/TSS
      RETURN
      END



      SUBROUTINE MOMPL(M,NPL,MD,D)
C     THIS SUBROUTINE CALCULATE SCATTERING MATRICES FOR POLAR AND
C     LONGITUDINAL POLARIZATIONS
C     LAYER MD IS BEFORE OR AFTER THE MAGNETIC LAYER IF<M OR >M,
C     RESPECTIVELY
      DIMENSION CT(30),N(30),ST(30)
      IMPLICIT COMPLEX (P,R,T)
      DIMENSION RPP(2),RSS(2),TPP(2),TSS(2),RSP(2),RPS(2),TSP(2),TPS(2)
      REAL LAMBDA,N,PI
      COMPLEX NCM11,NCM22,NCM12,NCM21,NM,CTM,EM1(4,4),CX,STM,
     1DELPP,DELSS,Q
      COMMON /DI/LAMBDA,N,Q,DUM(30),NM/PLTF/EM1,CT,ST,CTM,STM
      NCM12=N(MD)*CTM
      NCM11=N(MD)*CT(MD)
      NCM22=NM*CTM
      NCM21=NM*CT(MD)
      PHI=2.*PI()*D*N(MD)*CT(MD)/LAMBDA
      IF(MD.LT.M) PHI=2.*PI()*D*NM*CTM/LAMBDA
      CX=(0.,1.)*PHI
```

```
      PSI=PI()*NM*Q*DUM(M)/LAMBDA
      PRP=CEXP(CX)
      PRPN=CEXP(-CX)
      IF(MD-M) 5,5,10
5     K1=2
      K2=1
      GO TO 15
10    K1=1
      K2=2
15    RPP(K1)=(NCM21-NCM12)/(NCM21+NCM12)
      RSS(K1)=(NCM11-NCM22)/(NCM11+NCM22)
      TPP(K1)=N(MD)*(1.+RPP(K1))/NM
      TSS(K1)=1.+RSS(K1)
      RPP(K2)=-RPP(K1)
      RSS(K2)=-RSS(K1)
      TPP(K2)=NM*(1.-RPP(K1))/N(MD)
      TSS(K2)=1.-RSS(K1)
      RSP(K1)=(0.,0.)
      IF(NPL .EQ. -1) GO TO 1
      IF(CT(MD) .EQ. 0.) GO TO 2
      RSP(K1)=(0.,.25)*Q*TPP(K1)*TSS(K1)*NM/(CT(MD)*N(MD))
      GO TO 2
1     PSI0=PSI
      PSI=PSI0*STM/CTM
      IF(CT(MD).EQ.0.) GO TO 2
      RSP(K1)=(0.,.25)*Q*TPP(K1)*TSS(K1)*ST(MD)/(CT(MD)*CTM)
2     RPS(K1)=NPL*RSP(K1)
      TSP(K1)=RSP(K1)
      TPS(K1)=(N(MD)/NM)*(1.-NPL*(2.*CTM*CT(MD))/TPP(K1))*RPS(K1)
      TAUPP=(TPP(K2)*TPS(K1)-RPP(K2)*RPS(K1))
      TAUSS=(TSS(K2)*TSP(K1)-RSS(K2)*RSP(K1))
      DELPP=1.-RPP(K2)**2
      DELSS=1.-RSS(K2)**2
      IF(MD-M) 20,20,25
20    PSI0=PSI
      PSI=CSIN(PSI0)
      RCS=CCOS(PSI0)
      GO TO 30
25    PSI=(0.,0.)
      RCS=(1.,0.)
30    R1=(0.,0.)
      CALL CSCLA(EM1,R1,4,4,0)
      EM1(1,1)=RCS*PRP/TPP(2)
      EM1(1,3)=RCS*PRPN*RPP(2)/TPP(2)
      EM1(2,2)=RCS*PRP/TSS(2)
      EM1(2,4)=RCS*PRPN*RSS(2)/TSS(2)
      EM1(3,1)=RCS*PRP*RPP(2)/TPP(2)
      EM1(3,3)=RCS*PRPN/TPP(2)
      EM1(4,2)=RCS*PRP*RSS(2)/TSS(2)
      EM1(4,4)=RCS*PRPN/TSS(2)
      IF(MD-M) 33,35,40
35    EM1(1,2)=PRP*PSI/TPP(2)
      TOP=TPP(2)*RPS(2)-TPS(2)*RPP(2)
```

```
      EM1(1,4)=(RCS*TOP/(TPP(2)*TSS(2))-RPP(2)*PSI/TPP(2))*PRPN
      EM1(2,1)=-PRP*PSI/TSS(2)
      TOP=RCS*RSP(2)+RSS(2)*TPP(2)*PSI
      EM1(2,3)=PRPN*TOP/(TPP(2)*TSS(2))
      EM1(3,2)=PRP*RPP(2)*PSI/TPP(2)
      TOP=-(RCS*TPS(2)+TSS(2)*PSI)
      EM1(3,4)=PRPN*TOP/(TPP(2)*TSS(2))
      EM1(4,1)=-PRP*RSS(2)*PSI/TSS(2)
      TOP=TPP(2)*PSI-TSP(2)*RCS
      EM1(4,3)=PRPN*TOP/(TPP(2)*TSS(2))
      GO TO 45
40    EM1(1,2)=-NPL*PRP*TAUPP/(DELSS*TPP(2))
      EM1(1,4)=-NPL*PRPN*RSS(2)*TAUPP/(DELSS*TPP(2))
      EM1(2,1)=-NPL*PRP*TAUSS/(DELPP*TSS(2))
      EM1(2,3)=-NPL*PRPN*RPP(2)*TAUSS/(DELPP*TSS(2))
      EM1(3,2)=NPL*PRP*RPS(1)/(DELSS*TPP(2))
      EM1(3,4)=NPL*PRPN*RPS(1)*RSS(2)/(DELSS*TPP(2))
      EM1(4,1)=NPL*PRP*RSP(1)/(DELPP*TSS(2))
      EM1(4,3)=NPL*PRPN*RPP(2)*RSP(1)/(DELPP*TSS(2))
45    CONTINUE
      RETURN
      END



      SUBROUTINE MOMT(M,MD,D)
C     THIS SUBROUTINE CALCULATES SCATTERING MATRICES FOR TRANSVERSE
C     POLARIZATION
      DIMENSION CT(30),N(30),ST(30)
      IMPLICIT COMPLEX (P,R,T)
      DIMENSION RPP(2),RSS(2),TPP(2),TSS(2)
      REAL LAMBDA,N,PI
      COMPLEX PHI,NCM11,NCM22,NCM12,NCM21,NM,CTM,EM1(4,4),CX,BRA,STM,Q
      COMMON /DI/LAMBDA,N,Q,DUM(30),NM/PLTF/EM1,CT,ST,CTM,STM
      NCM12=N(MD)*CTM
      NCM11=N(MD)*CT(MD)
      NCM22=NM*CTM
      NCM21=NM*CT(MD)
      PHI=2.*PI()*D*N(MD)*CT(MD)/LAMBDA
      IF(MD.LT.M) PHI=2.*PI()*D*NM*CTM/LAMBDA
      CX=(0.,1.)*PHI
      PRP=CEXP(CX)
      PRPN=CEXP(-CX)
      IF(MD.GT.M) Q=-Q
      BRA=1.+(0.,1.)*Q*STM/CTM
      IF (MD-M) 5,5,10
5     K1=2
      K2=1
      GO TO 15
10    K1=1
      K2=2
15    RPP(K1)=(NCM21*BRA-NCM12)/(NCM21*BRA+NCM12)
```

```
      RSS(K1)=(NCM11-NCM22)/(NCM11+NCM22)
      TPP(K1)=N(MD)*(1.+RPP(K1))/NM
      TSS(K1)=1.+RSS(K1)
      RPP(K2)=(BRA*NCM12-NCM21)/(NCM21+NCM12*((2.,0.)-BRA))
      RSS(K2)=-RSS(K1)
      TPP(K2)=NM*(1.+RPP(K2))/N(MD)
      TSS(K2)=1.-RSS(K1)
      R1=(0.,0.)
      CALL CSCLA(EM1,R1,4,4,0)
      EM1(1,1)=PRP*(TPP(1)*TPP(2)-RPP(1)*RPP(2))/TPP(2)
      EM1(1,3)=PRPN*RPP(2)/TPP(2)
      EM1(2,2)=PRP/TSS(2)
      EM1(2,4)=PRPN*RSS(2)/TSS(2)
      EM1(3,1)=-PRP*RPP(1)/TPP(2)
      EM1(3,3)=PRPN/TPP(2)
      EM1(4,2)=PRP*RSS(2)/TSS(2)
      EM1(4,4)=PRPN/TSS(2)
      RETURN
      END



      SUBROUTINE MOOUT(NENT,IN)
C     THIS SUBROUTINE CALCULATES DESIRED QUANTITIES FROM SCATTERING
C     MATRIX; ALSO CONTROLS PRINT-OUT.
      IMPLICIT COMPLEX (R)
      COMPLEX S(4,4),NM,ZI,D1T(4,4),D2T(4,4),SP(4,4),SD(4,4),Q,Z
      REAL LAMBDA,N(30),RRLP2,RPPT2,RPPP2,RPPN2,NM1,NM2
      REAL*8 DDENT(5),POL(3)
      DIMENSION D(30),ST(30),CT(30),DT(3),DRAY(12),DD(4)
      DIMENSION RPP(101),RPS(101),RSP(101),RSS(101),RRLP2(101),
     1DPHIP(101),EPS(101),DREFL(101),RPPT2(101),DPHIT(101),DELRP(101)
     2,RPPP(101),RPPN(101)
      DATA POL/'LONG.','TRANSV.','POLAR'/
      DATA DRAY/'D(MA','G) (','MU)','D(M-','1) (','MU)',
     1'THET','A (D','EG)','D(M+','1) (','MU)'/
      COMMON /DI/LAMBDA,N,Q,D,NM/PLTF/RDUM(4,4),CT,ST,CTM,STM
      COMMON /INOUT/NFO,MO,LO,NTH,DTHO,THETAD,MTH,DELMD,NOUT,NLTP
     1,ARRPLT/RRLP2,DPHIP,EPS,DREFL,XO/ID/DDENT,DT,JPLOT/SOUT/S,DD,NXD
      EQUIVALENCE (RPP(1),RPPP(1)),(RPS(1),RPPN(1)),(RRLP2(1),RPPT2(1)
     1),(DPHIP(1),DPHIT(1)),(EPS(1),DELRP(1),
      GO TO (1,2,3) NENT
C     PRINT INPUT DATA
1     CONTINUE
      F1(Z)=AIMAG(Z)/REAL(Z)
      F2(Z)=ATAN(F1(Z))
      M=MO
      L=LO
      NM1=REAL(NM)
      NM2=AIMAG(NM)
      NF=NFO+1
      DLA(1)=D(L)*(MTH-1)*DELMD
```

```
      CALL DATE(DT)
      PRINT 5,DT,DDENT
5     FORMAT(////// DATE: ',2A4,A1/1X,5A8//)
      PRINT 30,THETAD,LAMBDA
      PRINT 35
      DO 60 J=1,NFO
      IF(J.EQ.L.AND.L.NE.M) PRINT 40,J,N(J),D(J),DLMAX
      IF(J.EQ.M.AND.J.NE.L) PRINT 45,J,NM1,NM2,D(J),Q
      IF(J.EQ.M.AND.J.EQ.L) PRINT 50,J,NM1,NM2,D(J),DLMAX,Q
      IF(J.NE.L.AND.J.NE.M) PRINT 55,J,N(J),D(J)
60    CONTINUE
C     CALCULATE PRINTOUT VARIABLES
      MNTH=MTH-NTH
      NXDO=0
      IF(M.GT.L) NXDO=1
      IF(M.LT.L) NXDO=3
      IF(L .EQ. 1) NXDO=2
      NXDT=1+3*NXDO
      NXDT2=2+NXDT
      NXD=1+NXDO
      JAP=0
C     RETURN IF ONLY GRAPHICS REQUESTED
      IF(NOUT .EQ.2) RETURN
      IF((M-NF) .EQ. 2) GO TO 8
      IF(NLTP .EQ. 0) GO TO 6
8     PRINT 1000,(DRAY(J), J=NXDT,NXDT2)
      PRINT 1100
      RETURN
6     PRINT 2000,(DRAY(J), J=NXDT,NXDT2)
      RETURN
7     CONTINUE
      JAP=JAP+1
      J=JAP
C     CALCULATE OUTPUT FOR POLAR OR LONGITUDINAL [illegible]
      RN=S(4,4)*S(1,3)-S(1,4)*S(4,3)
      RD=S(3,3)*S(4,4)-S(3,4)*S(4,3)
      RRP(J)=RN/RD
      [illegible]
```

```
306       RPP=0.5*(R1P+R2P)
          RLL=0.5*(R1P-R2P)
          RRL=0.5*(R1M-R2M)
          RLR=0.5*(R1M+R2M)
          GO TO 310
308       RRR=0.5*(R1P-ZI*R2M)
          RRL=0.5*(R1M+ZI*R2P)
          RLR=0.5*(R1M-ZI*R2P)
          RLL=0.5*(R1P+ZI*R2M)
310       RRL2=(CABS(RRL))**2
          RLR2=(CABS(RLR))**2
          RRLP2(J)=(0.5*CABS(R1M))**2
          DPHIP(J)=F2(RRL)-F2(RLR)
          EPS(J)=CABS(RRR/RLR)
          DREFL(J)=(RLR2-RRL2)/RRLP2(J)
          IF(NOUT .EQ. 2) RETURN
          PRINT 1200, DD(NXD),RPP(J),RPS(J),RSS(J),RSP(J)
          PRINT 1300, RRLP2(J),DPHIP(J),EPS(J),DREFL(J)
          RETURN
3         CONTINUE
C         CALCULATE OUTPUT FOR TRANSVERSE POLARIZATION
302       RN=S(4,4)*S(1,3)-S(1,4)*S(4,3)
          RD=S(3,3)*S(4,4)-S(3,4)*S(4,3)
          IF((M-NF),EQ,1) Q=-Q
          IF (IN .EQ. 1) GO TO 303
          JAR=JAR+1
          J=JAR
          RPPP(J)=RN/RD
          IN=1
          RETURN
303       RPPN(J)=RN/RD
304       CONTINUE
          IN=0
          RPPP2=(CABS(RPPP(J)))**2
          RPPN2=(CABS(RPPN(J)))**2
          RPPT2(J)=0.5*(RPPP2+RPPN2)
          DELRP(J)=(RPPP2-RPPN2)/RPPT2(J)
          DPHIT(J)=F2(RPPP(J))-F2(RPPN(J))
          IF(NOUT .EQ. 2) RETURN
          PRINT 2100, DD(NXD),RPPP(J),RPPN(J),RPPT2(J),DPHIT(J),DELRP(J)
          RETURN
30        FORMAT(' THETA  = ',F6.3,' DEG.',/,' LAMBDA = ',F6.3,' MICRONS
35        FORMAT(5X,'LAYER NO.',3X,'REFRACTIVE INDEX',11X,'THICKNESS
          1(MICRONS)')
40        FORMAT(9X,I2,11X,F6.3,11X,'DMIN = ',F7.4,3X,'DMAX = ',F7.4)
45        FORMAT(9X,I2,3X,'N = ',F6.3,2X,'K = ',F6.3,13X,F7.4,16X,'Q = ',
          1,2F9.4)
50        FORMAT(9X,I2,3X,'N = ',F6.3,2X,'K = ',F6.3,3X,'DMIN = ',F7.4,
          13X, DMAX = ',F7.4,3X,'Q = ',2F9.4)
55        FORMAT(9X,I2,11X,F6.3,21X,F7.4)
1000      FORMAT(1X,3A4,10X, RPP',25X,'RPS',25X,'RSS',25X,'RSP')
1100      FORMAT(2X,'R-L REFL',16X,'DELTA PHI(RAD)',17X,
```

```
     1'EPSILON',20X,'DELTA REFL(L)'/)
2000 FORMAT(//1X,3A4,9X,'RPPP',24X,'RPPN',16X,'P REFL',
     14X,'DELTA PHI(RAD)',2X,'DELTA REFL'/)
1200 FORMAT(1X,F7.5,2X,4(2E13.5,2X))
1300 FORMAT(20X,4(E13.5,15X))
2100 FORMAT(1X,F7.5,2X,2(2E13.5,2X),3(E12.5,2X))
     END



     SUBROUTINE MOPLOT(N,M,NO,L,DELX)
C    THIS SUBROUTINE CONTROLS THE GRAPHICS OUTPUT
C    ASSUMES MAXIMUM OF 100 INCREMENTS OF VARIABLE LAYER
     DIMENSION RRLP2(101),DPHIP(101),EPSRP(101),DREFL(101)
     1,DT(3),NY(9),RR(404),CAP1(15),XRAY(9)
     REAL*8 IDENT(5),YRAY(18)
     COMMON /ARRPLT/RRLP2,DPHIP,EPSRP,DREFL,XMIN/ID/IDENT,DT,JPLOT
     EQUIVALENCE (RR(1),RRLP2(1)),(CAP1(1),IDENT(1))
     DATA XRAY/'D(M-','1) (','MU)','D(MA','G) (','MU)','THET','A (D'
     1,'EG)'/
     DATA YRAY/'P:REFL',' ','DELTA PH','I-RAD-','DELTA RE','FL',
     1'FIGURE 0','F MERIT','R:L REFL',' ','DELTA PH','I-RAD-',
     2'EPSILON',' ','DELTA RE','FL','FIGURE 0','F MERIT'/
     DATA NY/6,14,10,15,8,14,7,10,15/
     IF(N .EQ. -1) N=1
     XMAX =1.00*(DELX*(M-1)+XMIN)
     GO TO (5,10) NO
5    DXP2=(XMAX-XMIN)/10.
C    SCLRND IS LOCAL ROUTINE FOR ROUNDING OFF NUMBERS
C    MAY BE OMITTED
     DXP2=SCLRND(DXP2)
     XMAX=XMIN+10.*DXP2
     GO TO 15
10   DXP2=(XMAX-XMIN)/9.
     DXP2=SCLRND(DXP2)
     XMAX=XMIN+9.*DXP2
15   JMAX=5
     IF(N .EQ. 0) JMAX=4
     DXP=0.5*DXP2
     DO 20 J=1,JMAX
     KY=8*IABS(N)+2*(J-1)+1
     KX=6*NO+3*L-5
     IMIN=(J-1)*101
     IF (J.EQ.JMAX) IMIN=0
     YMIN=1.
     YMAX=-1.
     MMAX=M
     IF(NO .EQ. 2) MMAX=M-1
     IF (J.LT.JMAX) GO TO 45
     DO 40 I=1,MMAX
40   RR(I)=RR(I+101)/(1.-RR(I))
45   CONTINUE
     DO 25 I=2,MMAX
```

```
      IF(I.EQ.MMAX) GO TO 35
      IMINI=IMIN+I
C     PREVENTS SPIKES CAUSED BY IMPRECISION IN RATIOS OF DIFFERENCES
      IF(ABS(RR(IMINI)-RR(IMINI-1)).GT.(10.*(ABS(RR(IMINI+1)-RR(IMINI-1)
     1)))) RR(IMINI)=0.5*(RR(IMINI+1)+RR(IMINI-1))
35    YMIN=AMIN1(YMIN,RR(IMIN+I))
25    YMAX=AMAX1(YMAX,RR(IMIN+I))
C     SIZE IS LOCAL ROUTINE FOR CHOOSING SCALES
C     NEXT FOUR STEPS MAY BE OMITTED
      IF(YMAX.NE.0.) YMAX=SIGN(1.,YMAX)*SIZE(ABS(YMAX))
      IF(YMAX .LT. 0.) YMAX =0.
      IF(YMIN.NE.0.) YMIN=SIGN(1.,YMIN)*SIZE(ABS(YMIN))
      IF(YMIN .GT. 0.) YMIN=0.
      DYP2=(YMAX-YMIN)/10.
      IF(.NOT.(YMIN.EQ.0..OR.YMAX.EQ.0.) .AND. YMAX.NE.(-YMIN))
     1DYP2=AMAX1(ABS(YMAX),ABS(YMIN))/10.
      DYP=0.5*DYP2
      CALL SPLOTS(7.00,5.,.75,.25,XMAX,YMAX,XMIN,YMIN)
      CALL BOX(0)
      CALL AXIS(2)
      CALL TICKS(DXP,DYP,.1)
      CALL SCALE(DXP2,DYP2)
      IF(JPLOT) 48,48,50
48    CALL TITLE(CAP1,49)
      GO TO 52
50    CALL TITLE(CAP1,40)
52    CALL XLABL(XRAY(KX),11)
      CALL YLABL(YRAY(KY),NY(4*N+J))
      DO 30 I=1,M
      X=(I-1)*DELX+XMIN
      Y=RR(IMIN+I)
      IPL=2
      IF (I .EQ. 1) IPL=3
30    CALL SPLOT(X,Y,IPL)
      CALL COPY
C     PAUSE() IS LOCAL ROUTINE FOR AVOIDING INSTRUMENTAL PROBLEM
      CALL PAUSE(10)
      CALL ALPHA
20    CONTINUE
      CALL CLEAR
      RETURN
      END
```

References

1. "The Laser Gyro," F. Aronowitz, in "Laser Applications," Vol. 1, ed. M. Ross (Academic Press, New York, 1971) p. 134.

2. "Magneto-Optic Materials for Biasing Ring Laser Gyros," "Report No. 1," J.J. Krebs, G.A. Prinz, D.W. Forester and W.G. Maisch, NRL Memorandum Report 3870, April, 1978; "Report No. 2" G.A. Prinz J.J. Krebs, W.G. Maisch and D.W. Forester, NRL Memorandum Report 4198, April, 1980.

3. "Applications of Magneto-Optics in Ring Laser Gyroscopes," J.J. Krebs, W.G. Maisch, G.A. Prinz and D.W. Forester, 1980 IEEE Intern. Magnetics Conf., IEEE Trans. Mag. **MAG-16** (1980), to be published.

4. "The SLIC-7 Laser Gyro Inertial Guidance System," R.F. Morrison, E. Levinson, and B.L. Bryant, Jr., Proc. 1977 IEEE Nat. Aerospace Electronics Conf. (IEEE, New York, 1977) p. 1045.

5. "An Improved Ring Laser Bias Element," R.E. McClure and E. Vaher, Proc. 1978 IEEE Nat. Aerospace Electronics Conf. (IEEE, New York, 1978) p. 544.

6. "Magneto-Optic Scattering from Thin Solid Films," R.P. Hunt, J. Appl. Phys. **38**, 1652 (1967).

7. "Magneto-Optical Scattering from Multi-layer Magnetic and Dielectric Films," D.O. Smith, "Part I. General Theory," Opta Acta **12**, 13 (1965); "Part II. "Applications of the General Theory." Opta Acta **12**, 193 (1965).

8. "An Electrical Equivalent Circuit for the Transverse Magneto-Optic Effect in Thin Magnetic Films," R.E. McClure, 1980 IEEE Intern. Magnetics Conf., IEEE Trans. Mag. **MAG-16** (1980), to be published.

9. "Electromagnetic Theory of the Kerr and the Faraday Effects for Oblique Incidence," C.C. Robinson, J. Opt. Soc. Amer. **54**, 1220 (1964).

10. "Ring Laser Magnetic Bias Mirror Compensated for Non-reciprocal Loss," W. Macek, U.S. Patent No. 3, 851, 973 (Dec. 3, 1974).

11. "A Manganese Bismuth Magnetic Mirror for the Raytheon Laser Gyroscope," T.A. Dorschner, I.W. Smith and H. Statz, Proc. 1978 IEEE Nat. Aerospace Electronics Conf. (IEEE, New York, 1978) p. 569.

12. "Fabrication of Thin Film Garnet Structures for Intra-Cavity Laser Applications," E.C. Whitcomb and R.D. Henry, J. Appl. Phys. **49**, 1803 (1978).

13. "Magneto-optical Characterization of Thin Films of $Fe_{1-x}B_x$, $Fe_{1-x}Si_x$ and Fe-overcoated Permalloy," J.J. Krebs, G.A. Prinz, D.W. Forester and W.G. Maisch, J. Appl Phys. **50**, 2449 (1979).

14. "Magneto-optic Investigations of MnBi Films," G. Lewicki and J.E. Guisinger, J. Appl. Phys. **44**, 2361 (1973).

15. "Determination of the Optical and Magneto-Optical Constants of Thin Film Manganese Bismuth in the Visible Spectrum," R. Atkinson and P.H. Lissberger, Int. J. Magnetism **6**, 227 (1974).

16. "Substituted Rare Earth Garnet Substrate Crystals and LPE Films for Magneto-optic Applications," M. Kestigian, W.R. Bekebrede and A.B. Smith, J. Crystal Growth **42**, 343 (1977). See also other papers on magnetic garnets given in Ref. 3.

17. The Q_1 and Q_2 values quoted here for Fe at 1.15 μm are a correction of those given in Ref. 3. Note that $|Q|$ is not affected by this correction and hence the results given in Ref. 3 remain valid.

FIGURE CAPTIONS

Figure 1 — A general magnetic-dielectric multilayer thin film structure.

Figure 2 — Simplified flow diagram for program MOFILM.

Figure 3 — Differential phase shift vs tuning layer thickness d_{M-1} for the Fe-based mirror design shown.

Figure 4 — Total reflectivity vs d_{M-1} for the Fe-based design shown.

Figure 5 — Differential reflectivity vs d_{M-1} for the Fe-based design shown.

Figure 6 — Figure of merit $\Delta\Phi/(1-R)$ vs d_{M-1} for the Fe-based design shown.

Figure 7 — Maximum phase shift vs optical loss for several Fe-based, transverse Kerr magnetic mirrors at 0.63μm.

Figure 8 — Differential phase shift vs d_{M-1} for the Fe-based design shown.

Figure 9 — Differential reflectivity vs d_{M-1} for the Fe-based design shown.

Figure 10 — Figure of merit vs d_{M-1} for the Fe-based design shown.

Figure 11 — Mode mixing vs d_{M-1} for the Fe-based design shown.

Figure 12 — Differential phase shift vs d_{M-1} for the MnBi-based design shown.

Figure 13 — Figure of merit vs d_{M-1} for the MnBi-based design shown.

Figure 14 — Differential phase shift vs the magnetic layer thickness d_M for the garnet-based design shown.

Figure 15 — Total reflectivity vs d_M for the garnet-based design shown.

Figure 16 — Differential reflectivity vs d_M for the garnet-based design shown ($Q_2 = 0$).

Figure 17 — Figure of merit vs d_M for the garnet-based design shown.

Figure 18 — Differential reflectivity vs d_M for the garnet-based design shown ($Q_2 = Q_1$).

Figure 19 — Differential phase shift vs d_M for the garnet-based design shown.

Figure 20 — Differential reflectivity vs d_M for the garnet-based design shown.

Figure 21 — Figure of merit vs d_M for the garnet-based design shown.

Figure 22 — Differential phase shift vs d_M for the Fe-based design shown.

Figure 23 — Reflectivity vs d_M for the Fe-based design shown.

Figure 24 — Differential reflectivity for the Fe-based design shown.

Figure 25 — Figure of merit vs d_M for the Fe-based design shown.

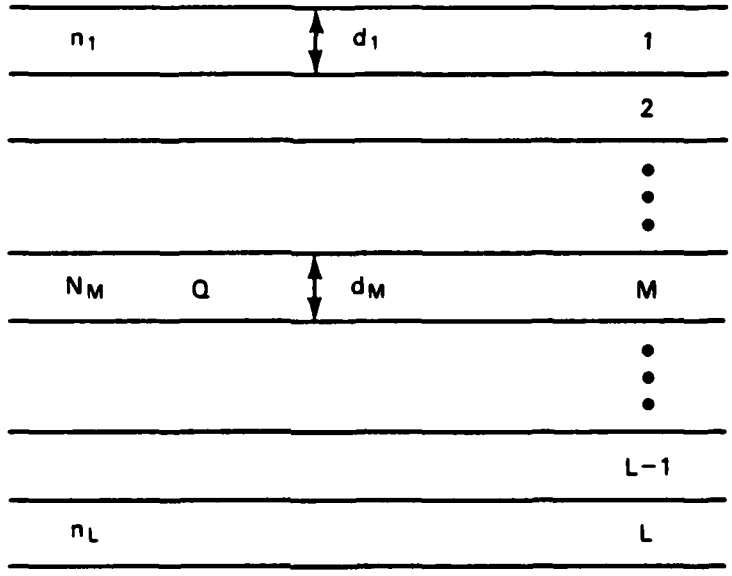

Figure 1 — A general magnetic-dielectric multilayer thin film structure

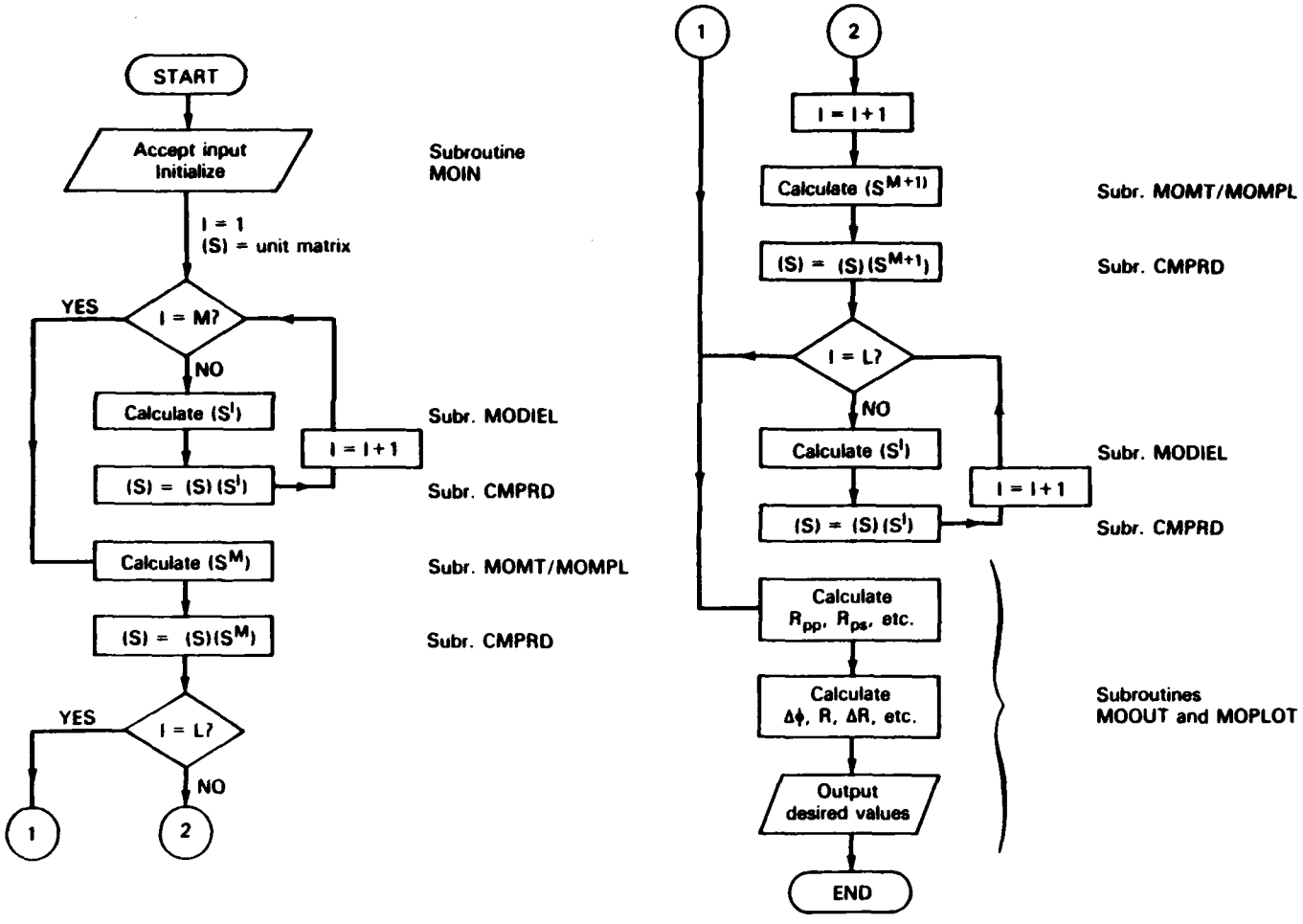

Figure 2 — Simplified flow diagram for program MOFILM

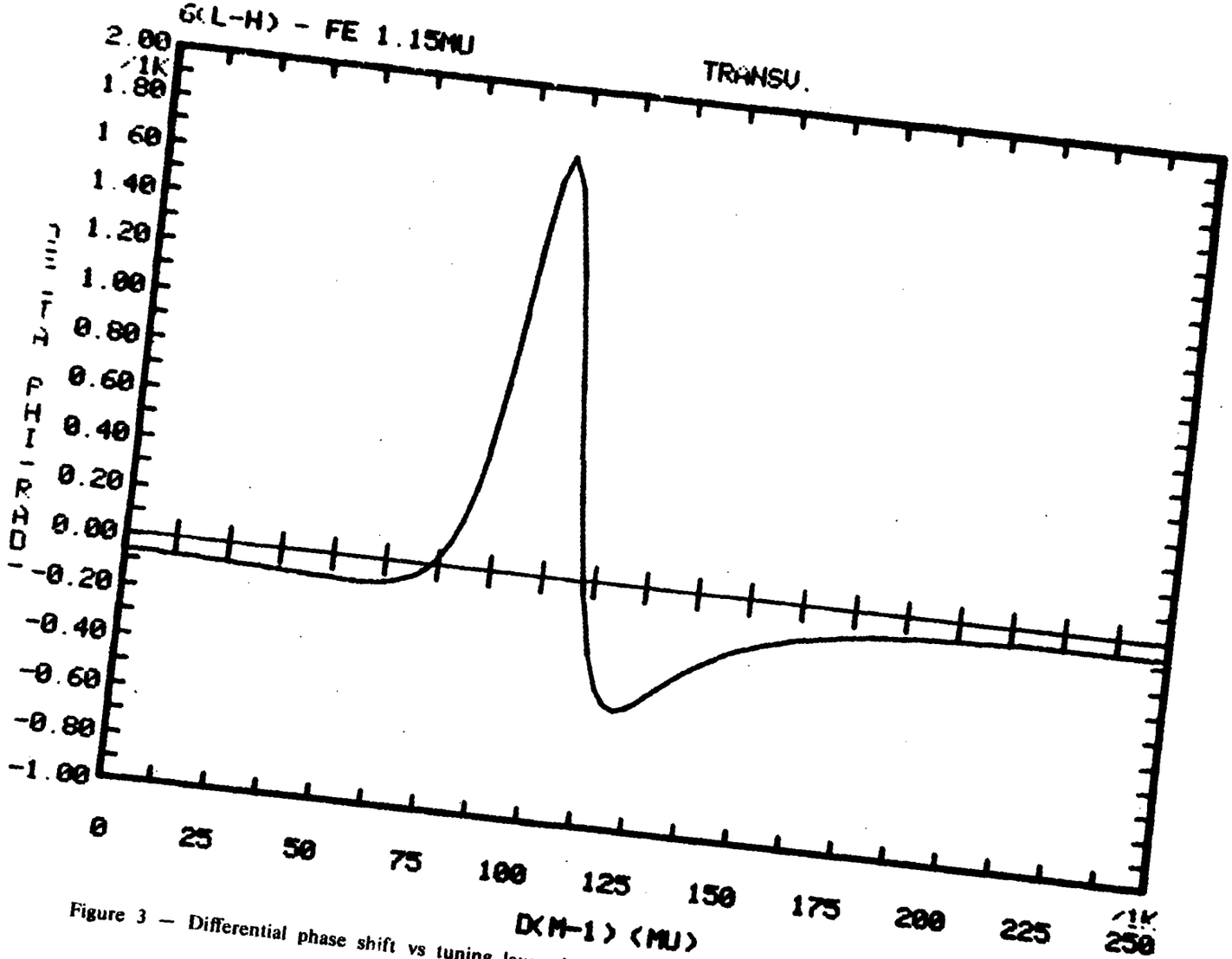

Figure 3 — Differential phase shift vs tuning layer thickness d_{M-1} for the Fe-based mirror design shown

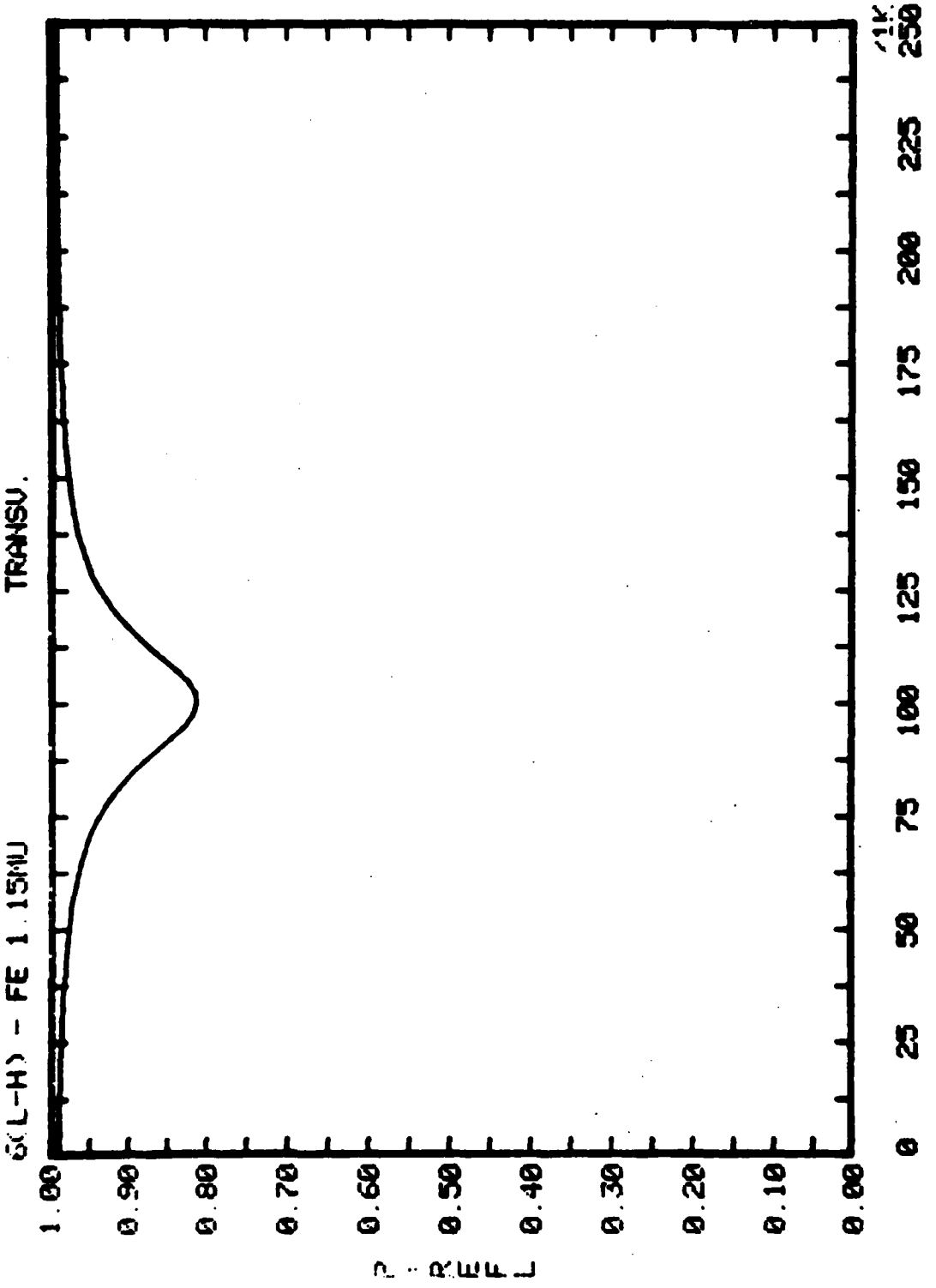

Figure 4 — Total reflectivity vs d_{M-1} for the Fe-based design shown

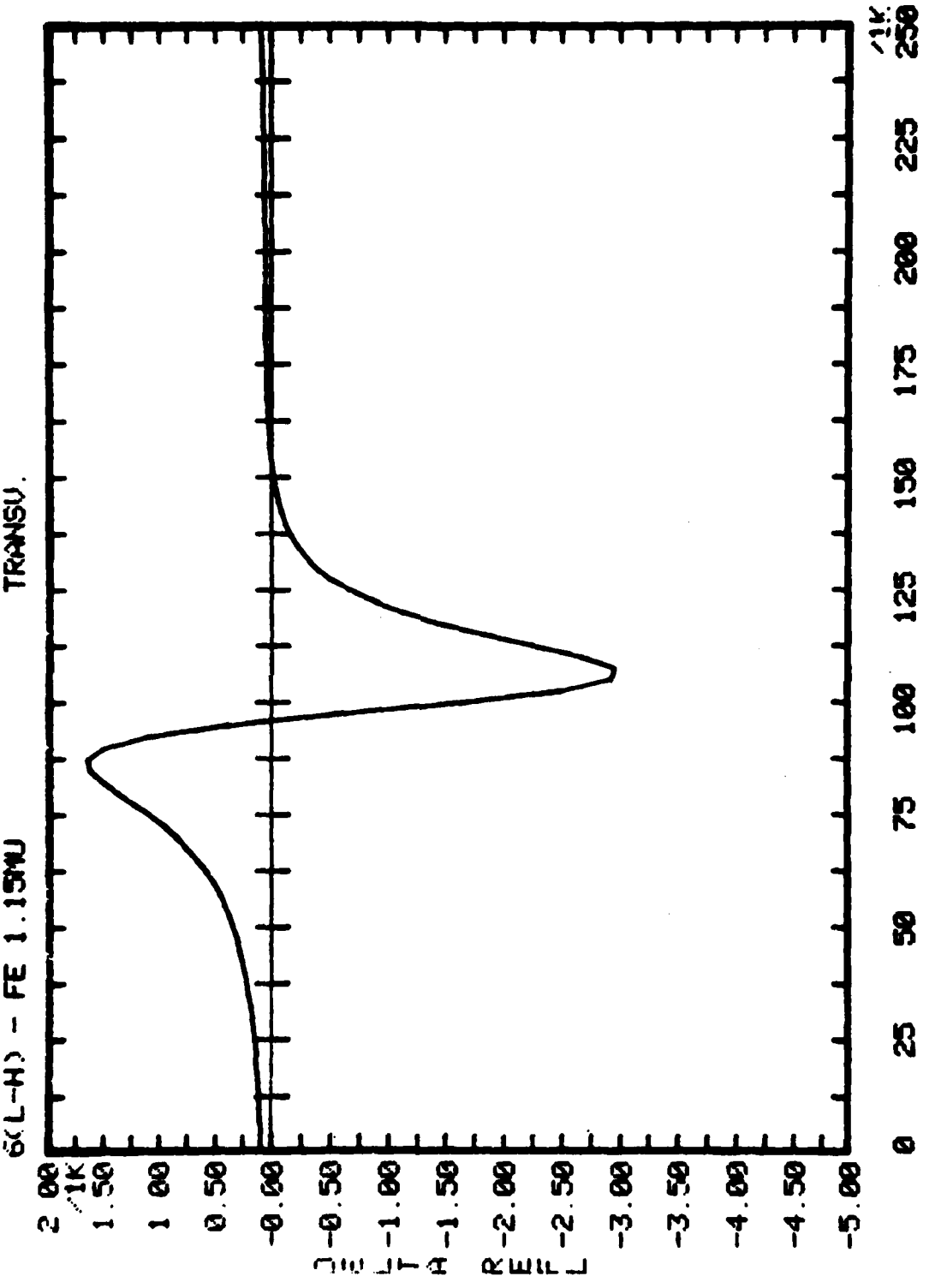

Figure 5 — Differential reflectivity vs d_{M-1} for the Fe-based design shown

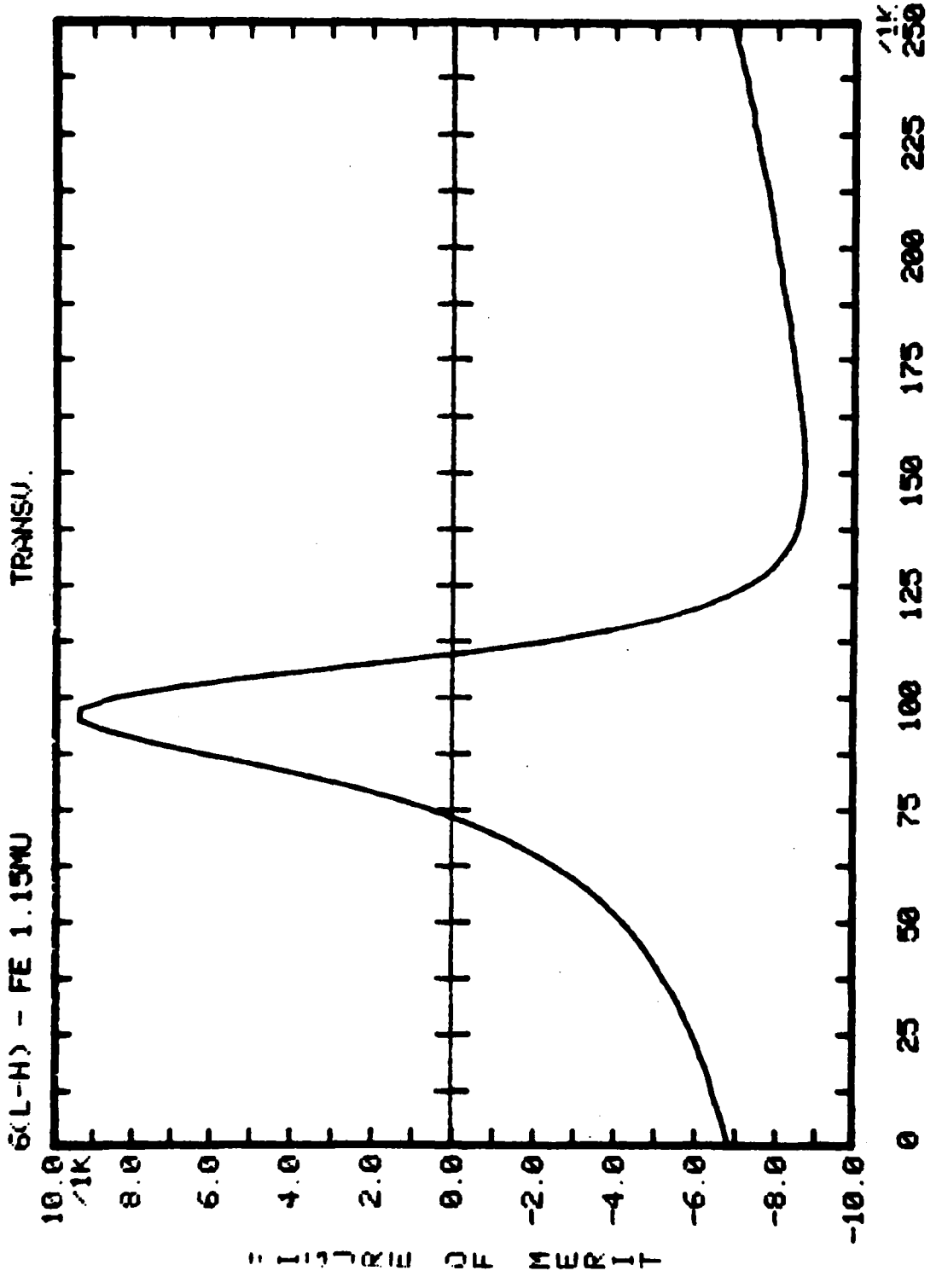

Figure 6 — Figure of merit $\Delta\Phi/(1-R)$ vs d_{M-1} for the Fe-based design shown

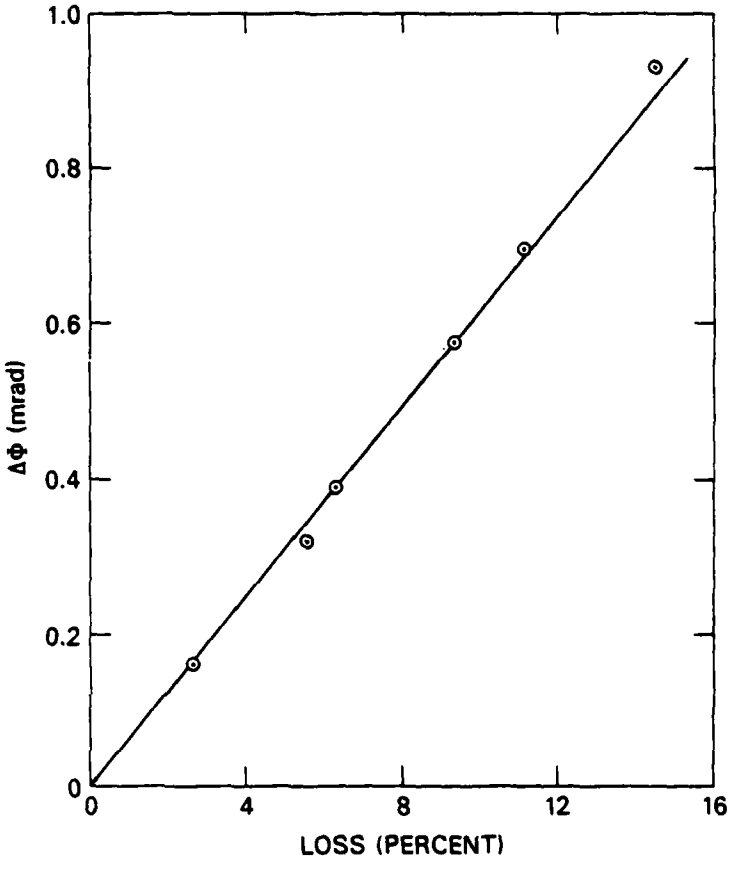

Figure 7 — Maximum phase shift vs optical loss for several Fe-based, transverse Kerr magnetic mirrors at 0.63μm

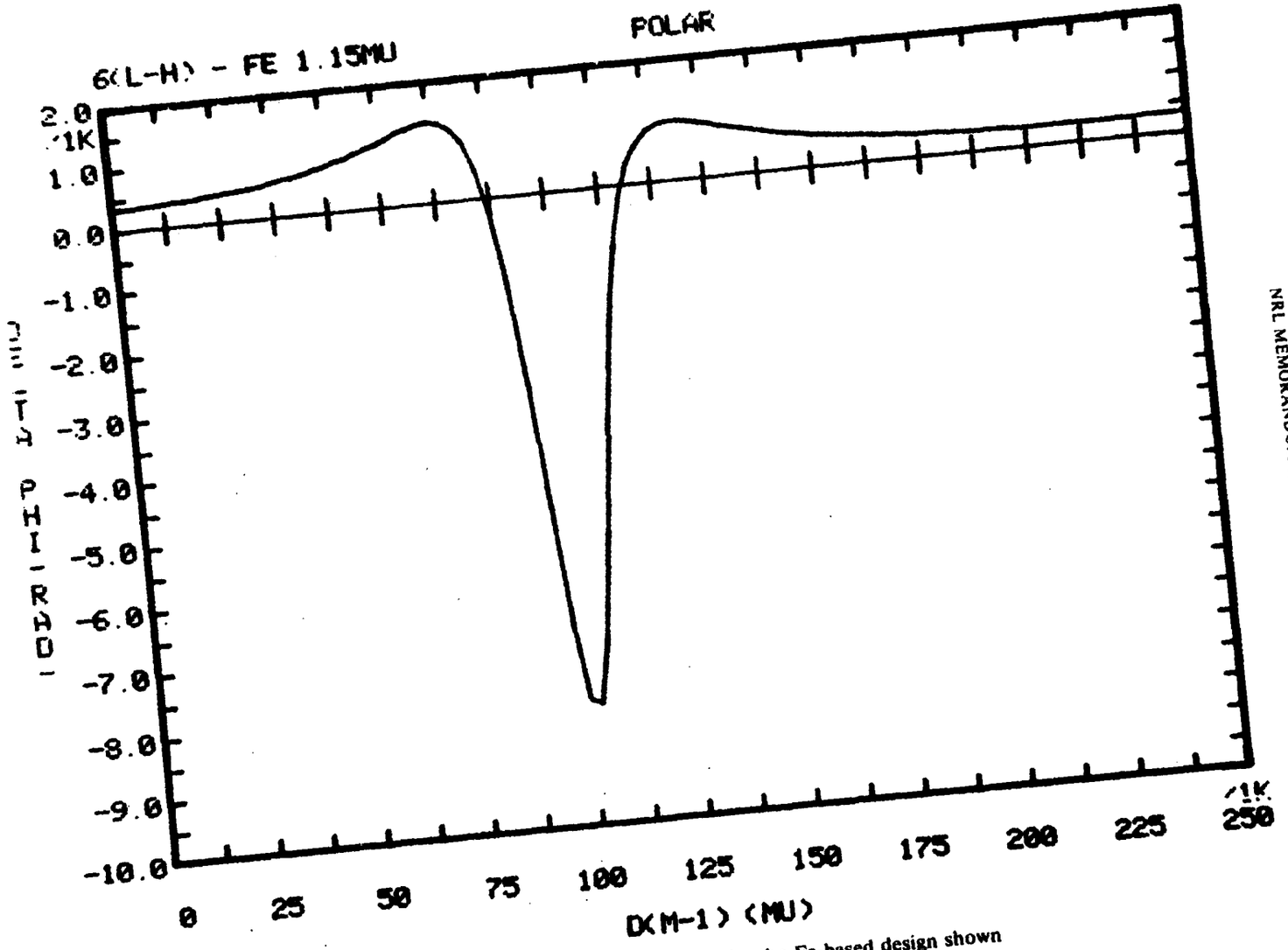

Figure 8 — Differential phase shift vs d_{M-1} for the Fe-based design shown

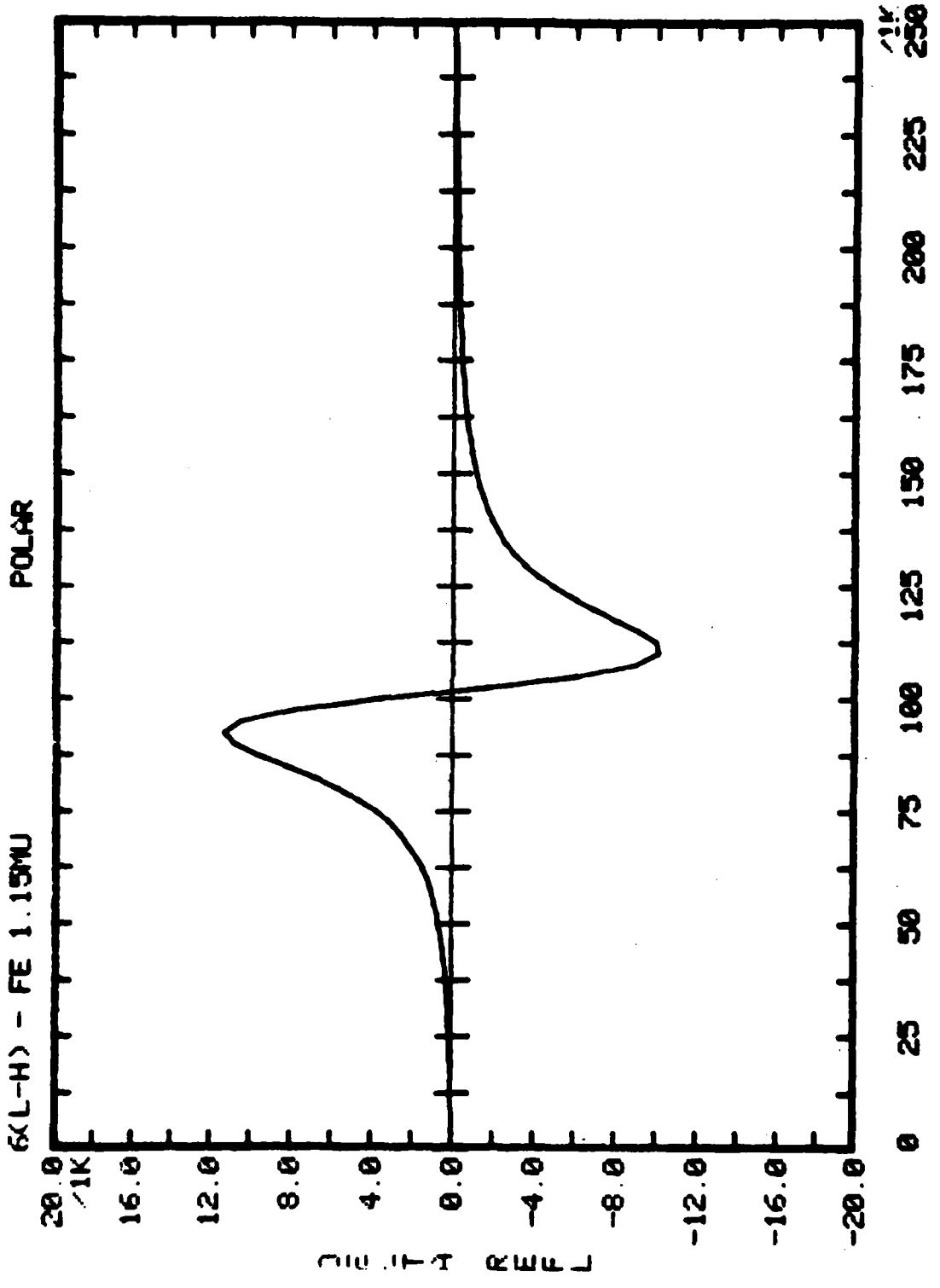

Figure 9 — Differential reflectivity vs d_{M-1} for the Fe-based design shown

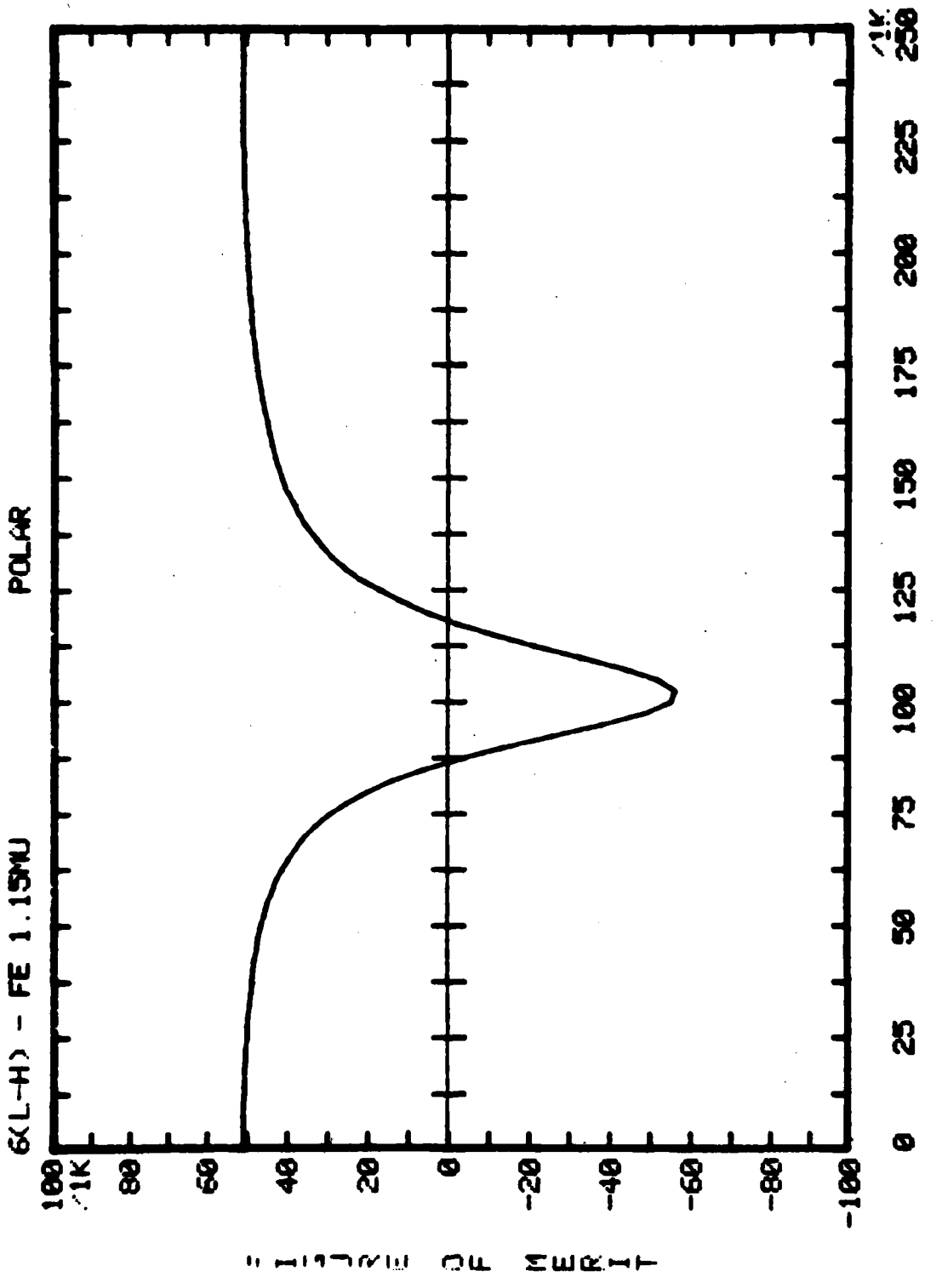

Figure 10 — Figure of merit vs d_{M-1} for the Fe-based design shown

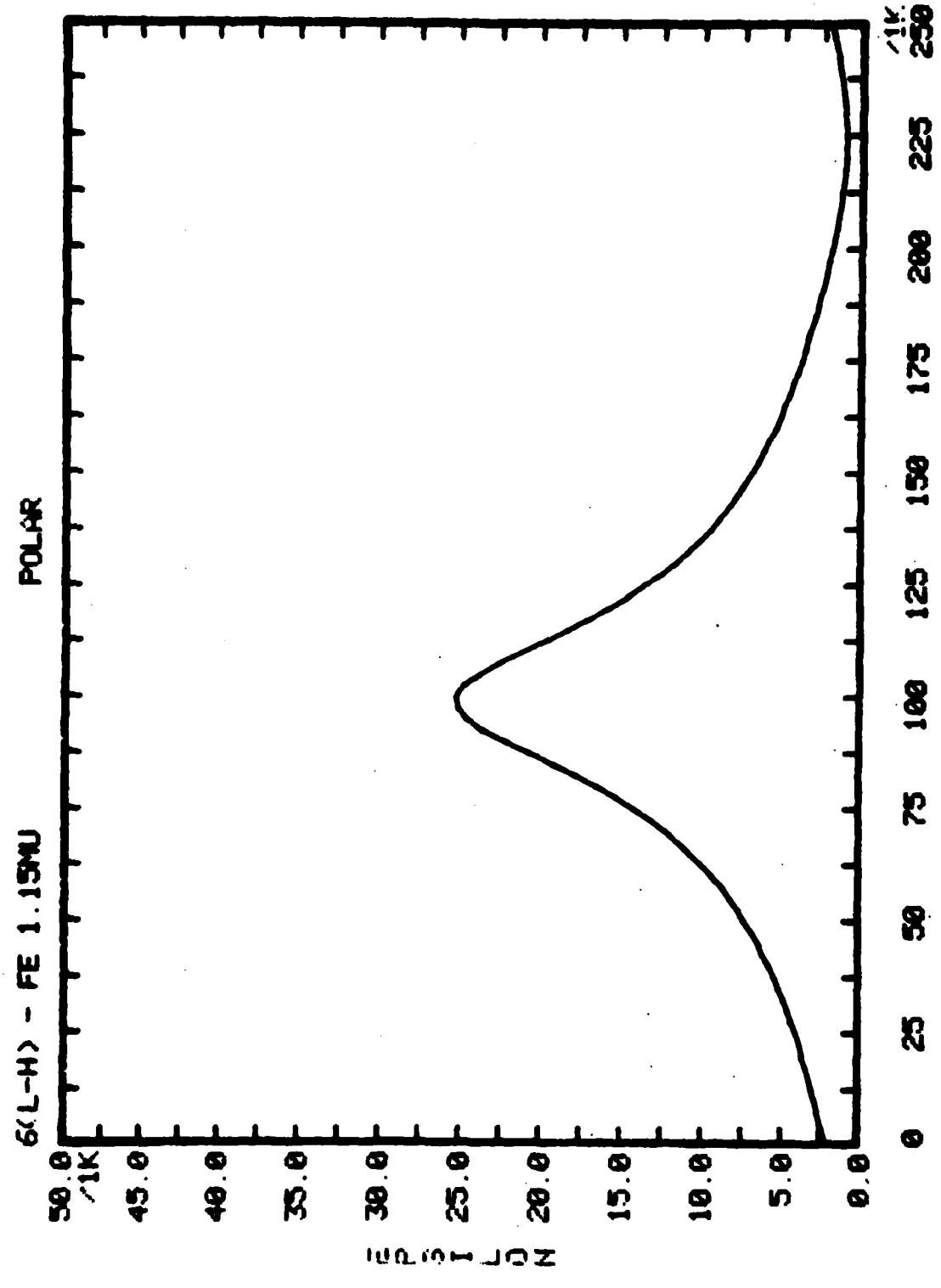

Figure 11 — Mode mixing vs d_{M-1} for the Fe-based design shown

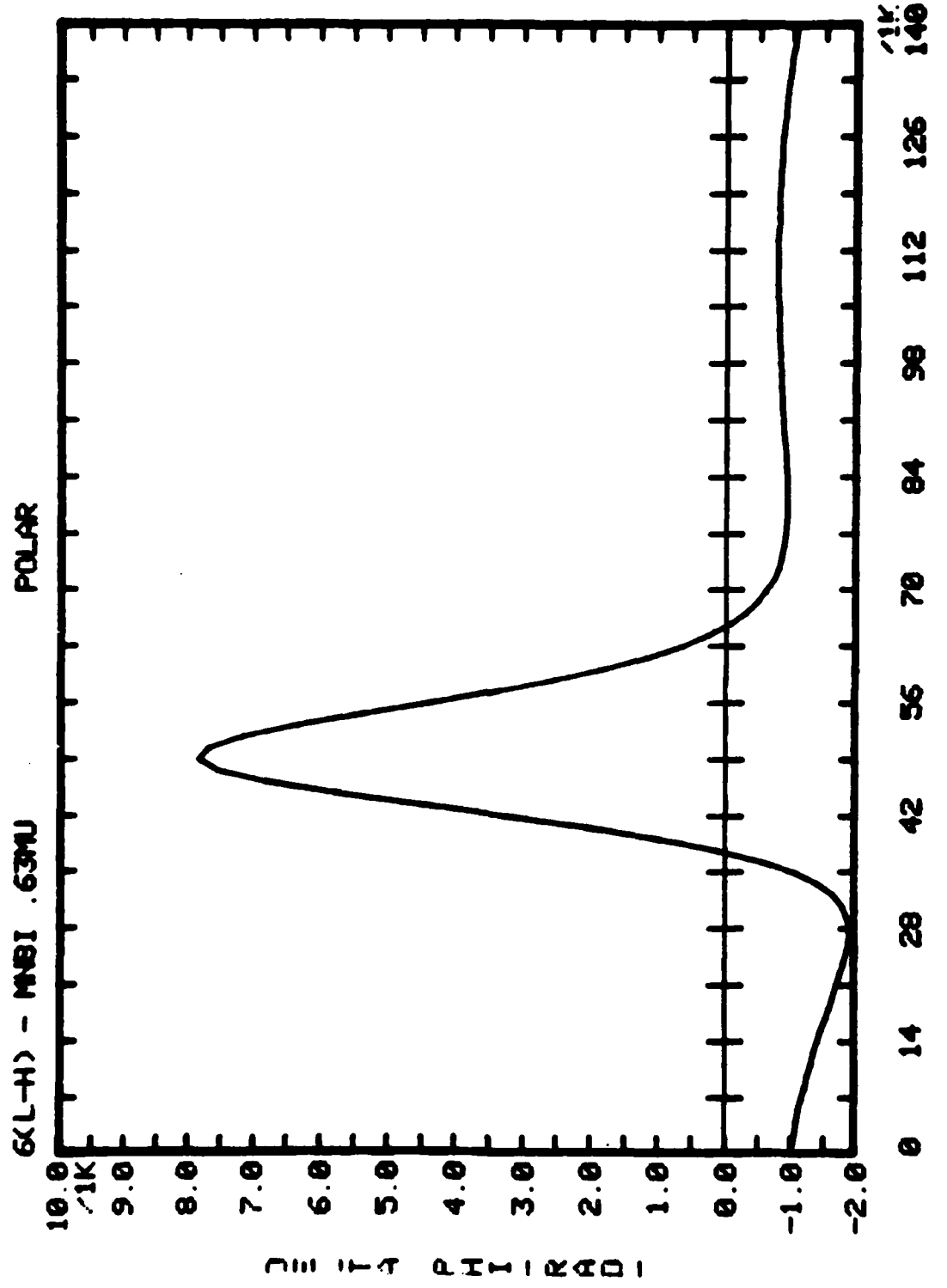

Figure 12 — Differential phase shift vs d_{M-1} for the MnBi-based design shown

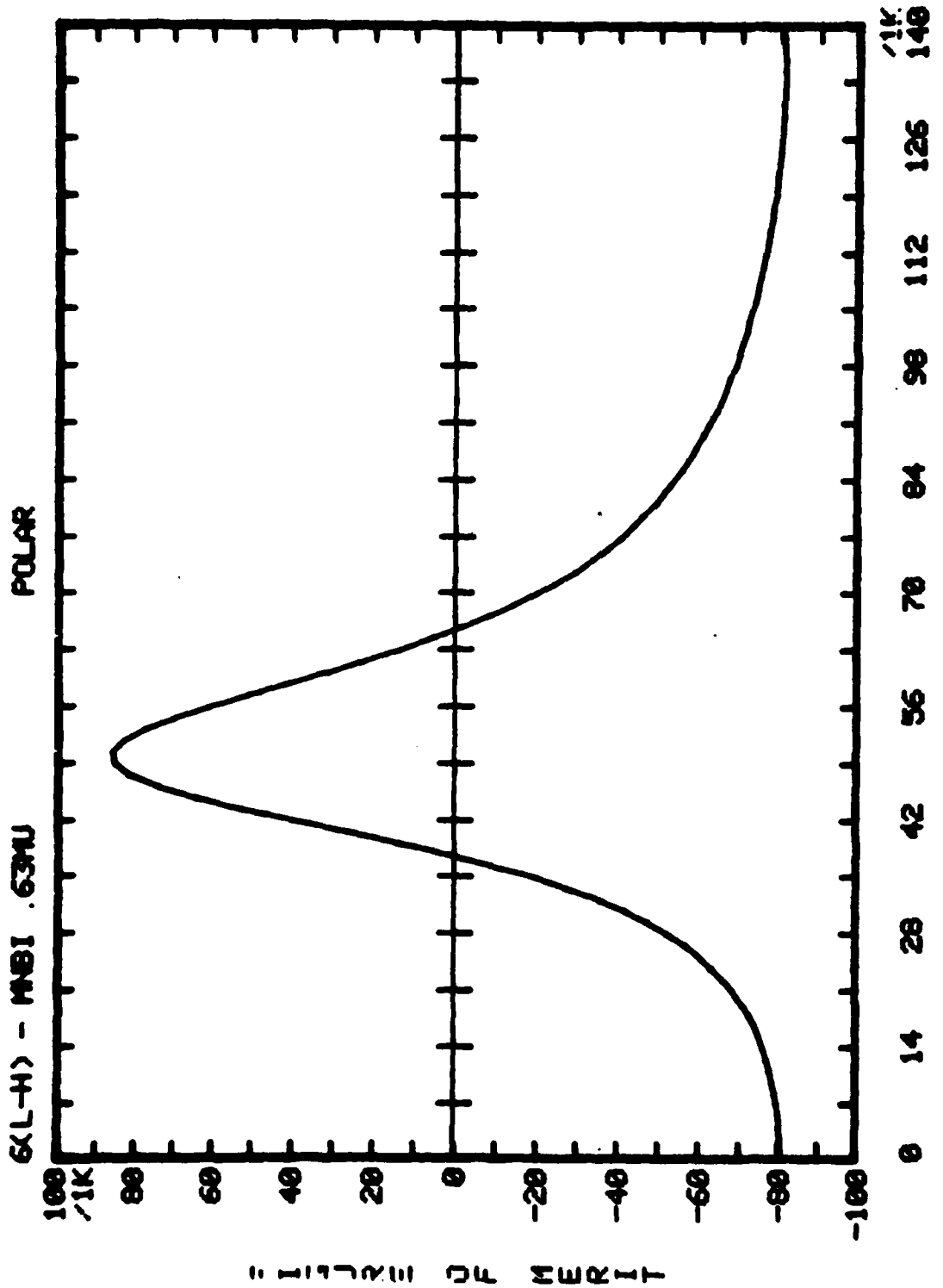

Figure 13 — Figure of merit vs d_{M-1} for the MnBi-based design shown

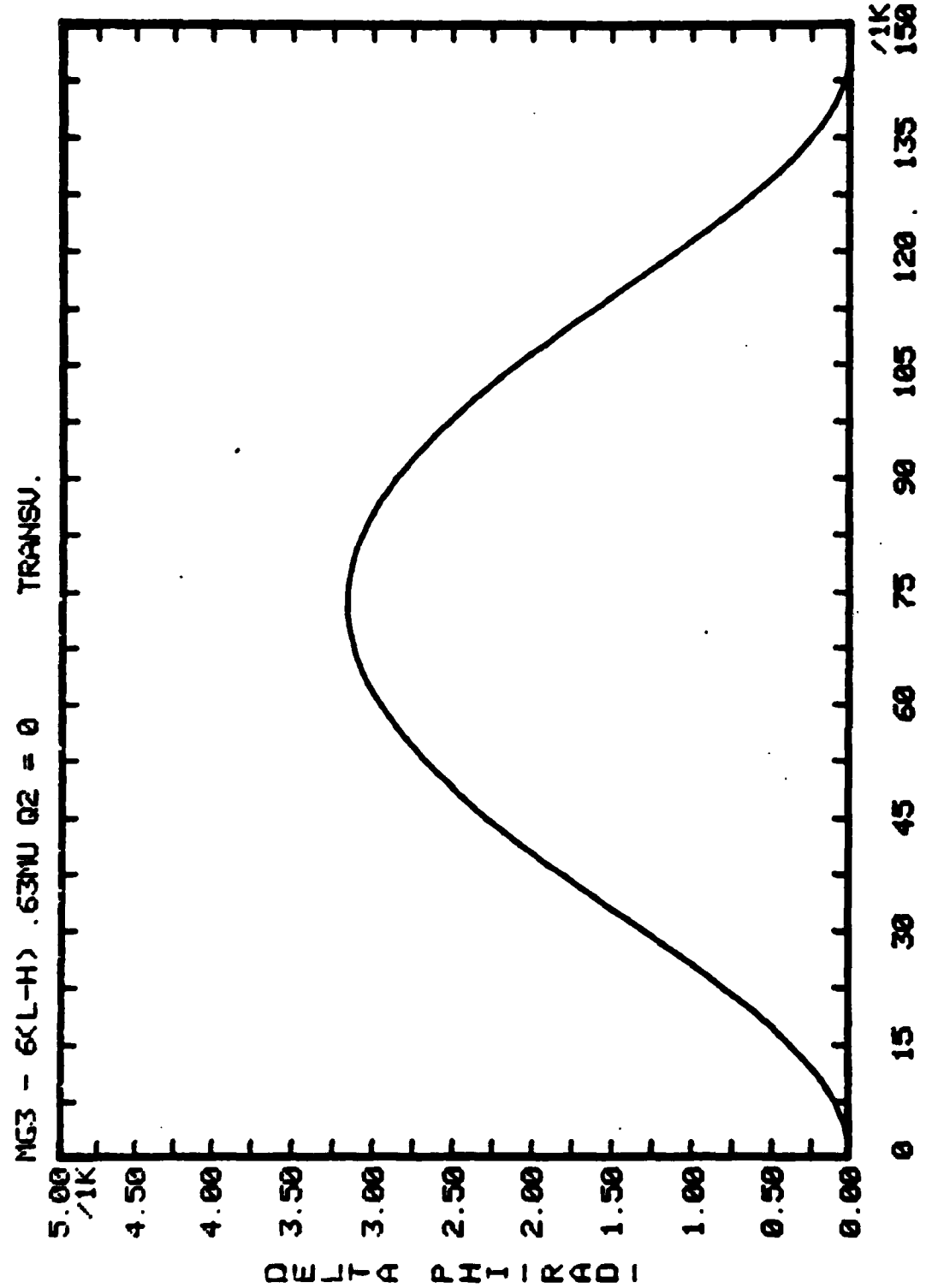

Figure 14 — Differential phase shift vs the magnetic layer thickness d_M for the garnet-based design shown

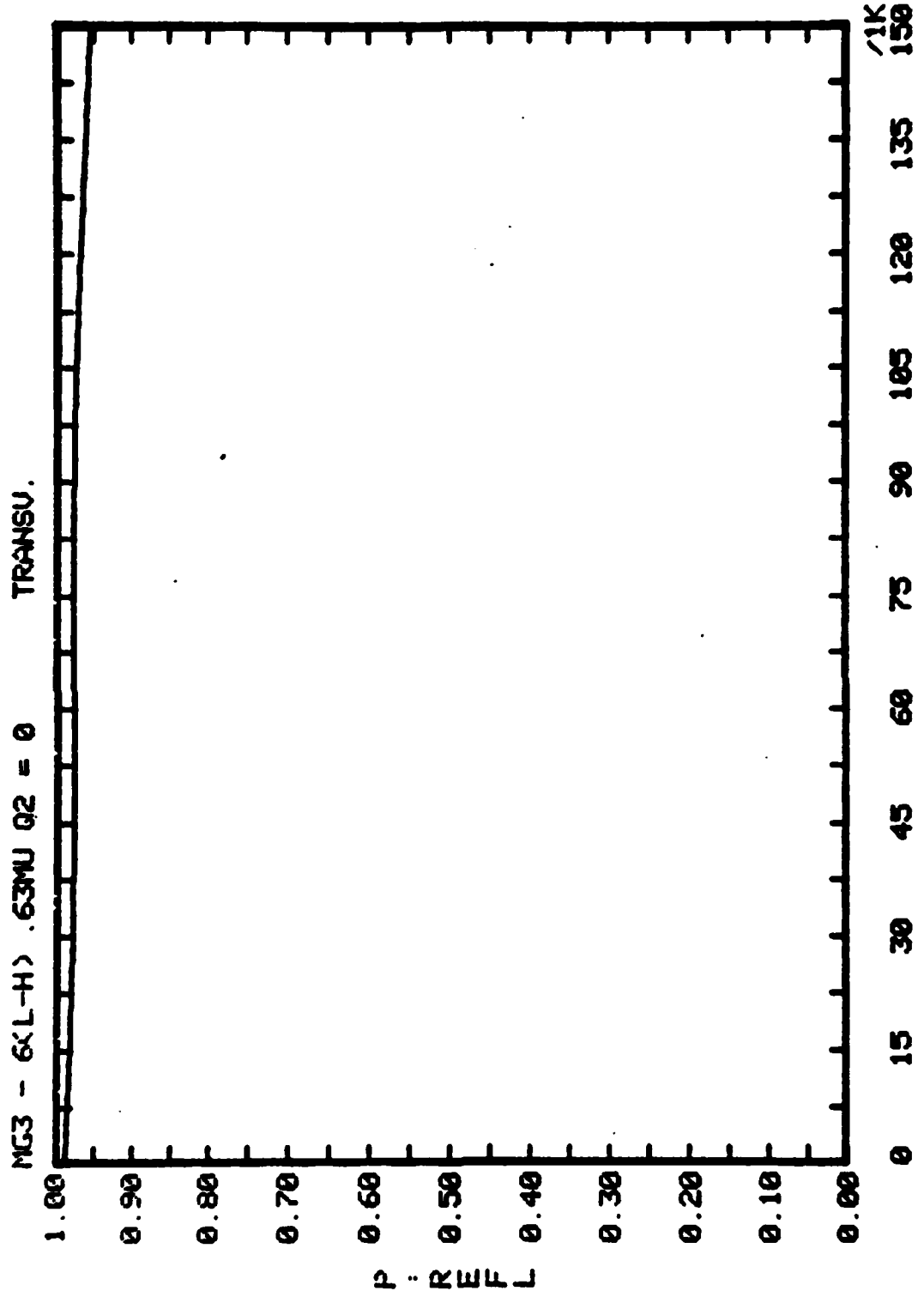

Figure 15 — Total reflectivity vs d_M for the garnet-based design shown

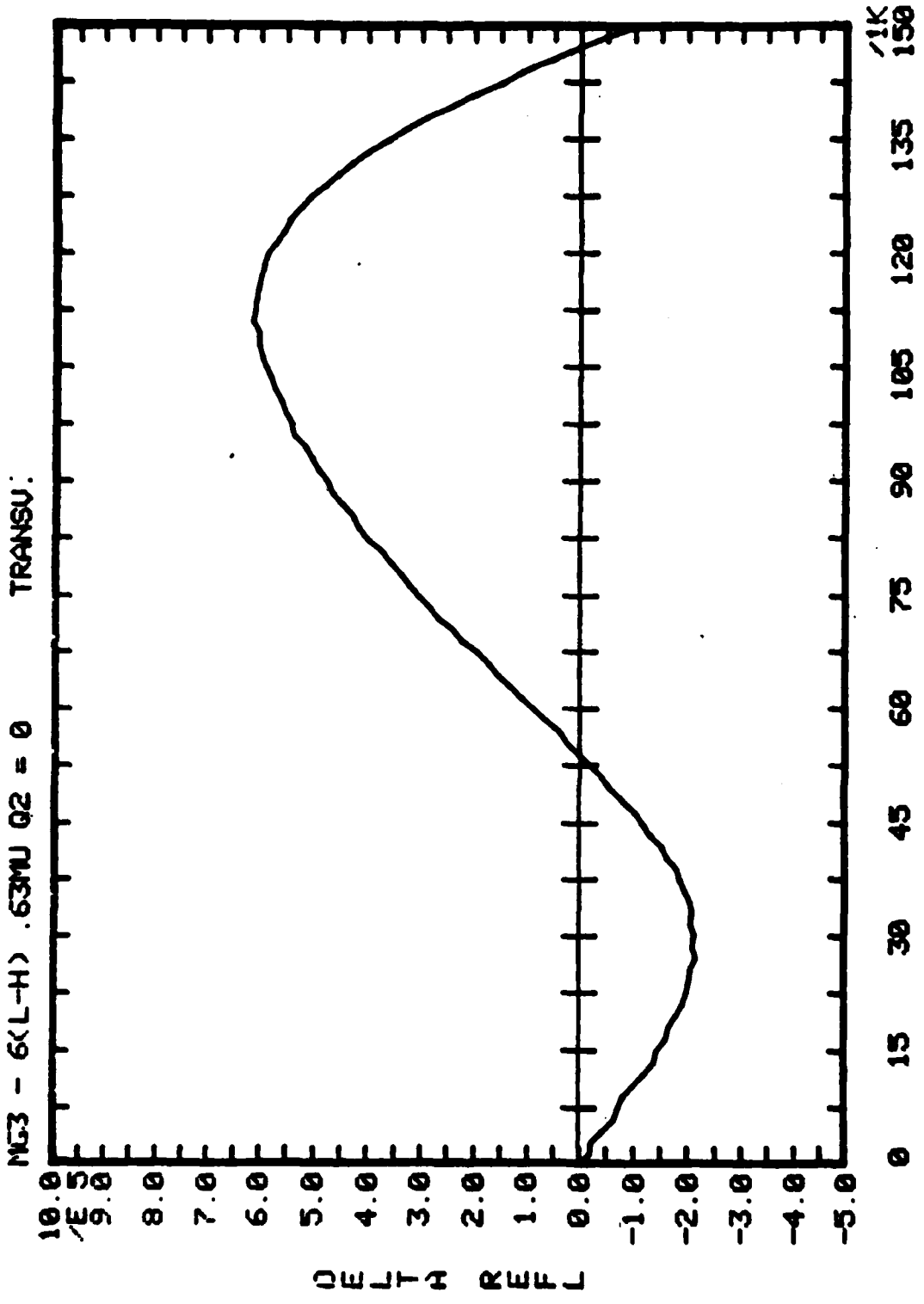

Figure 16 — Differential reflectivity vs d_M for the garnet-based design shown ($Q_2 = 0$)

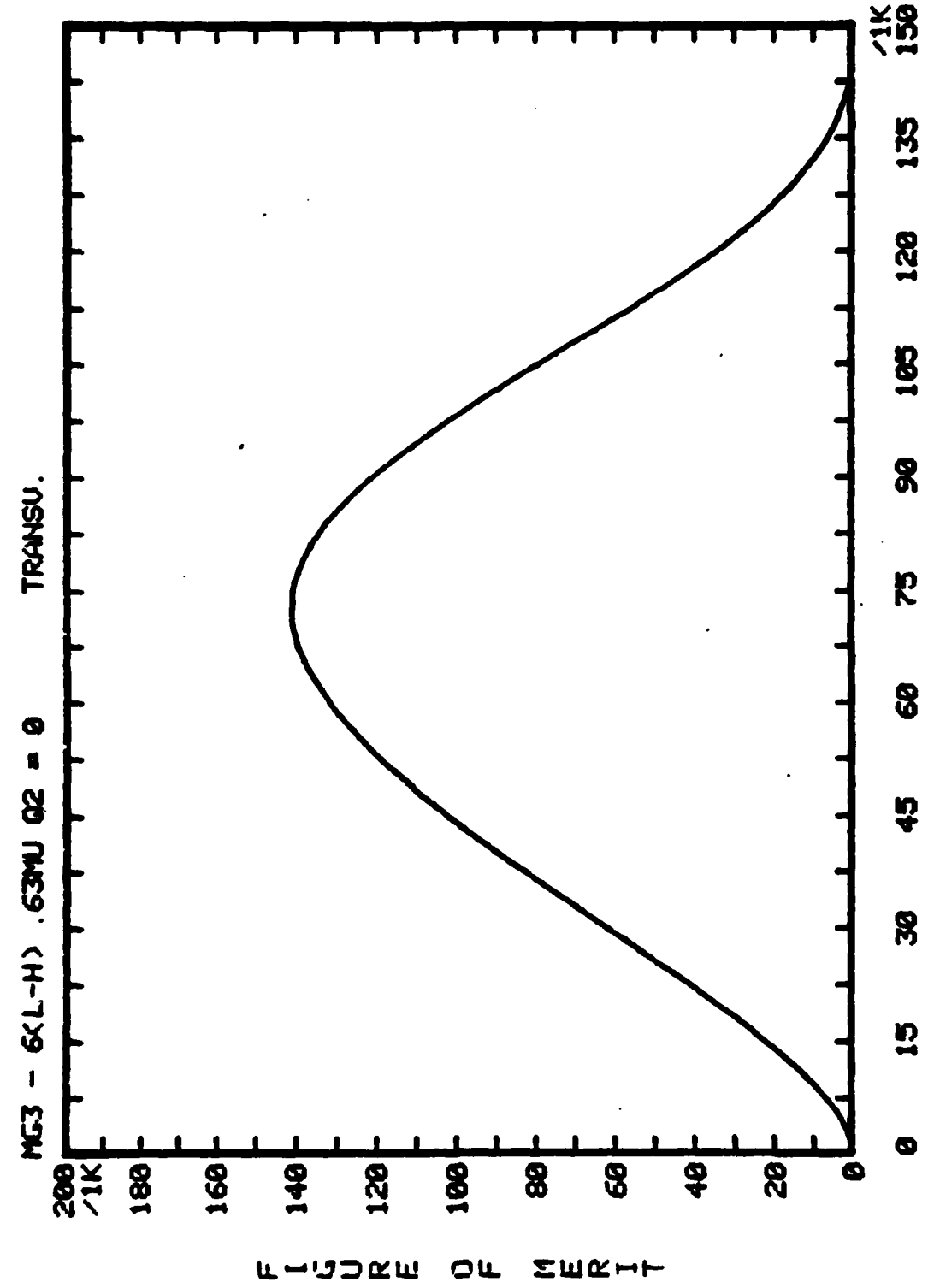

Figure 17 — Figure of merit vs d_M for the garnet-based design shown

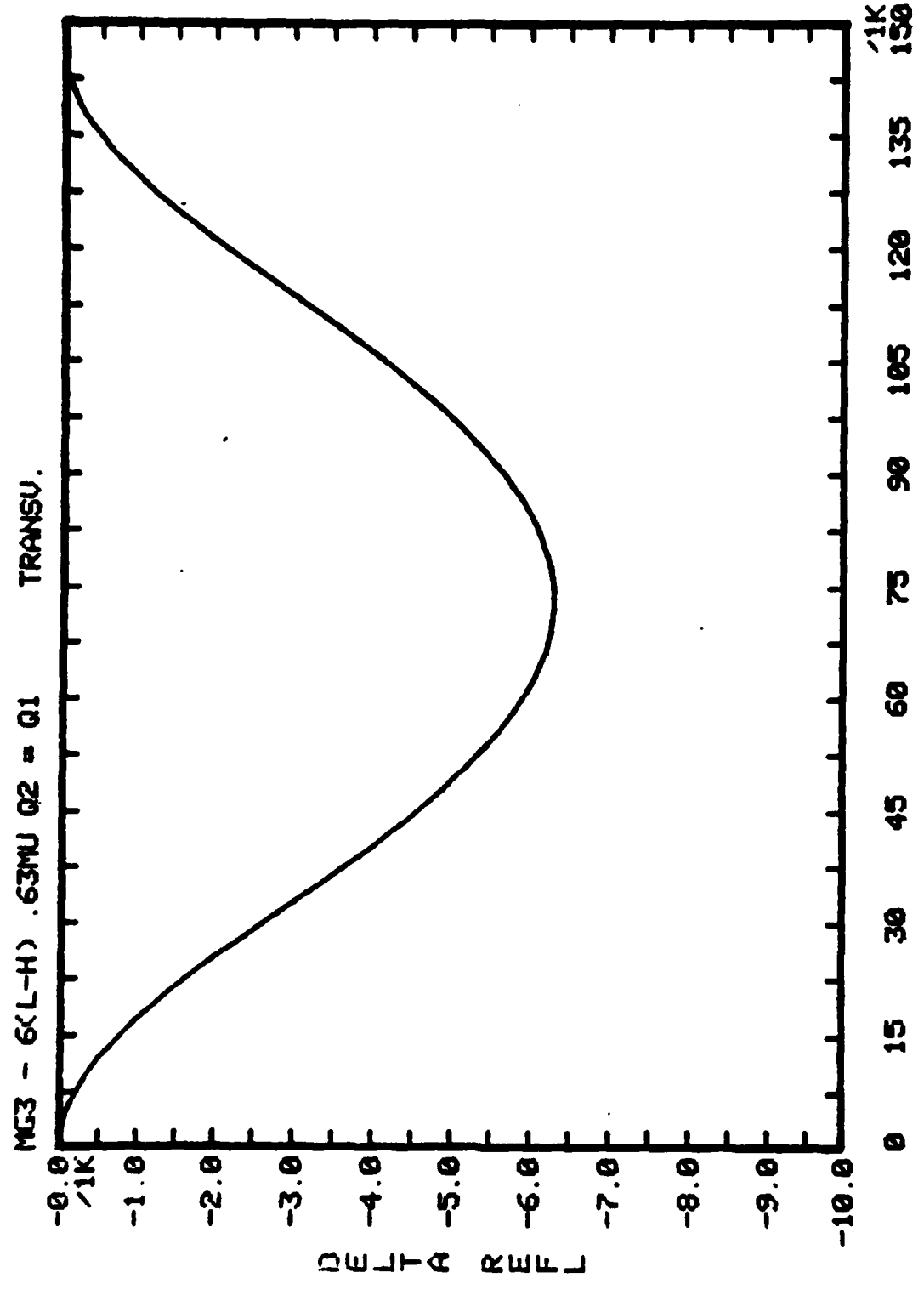

Figure 18 — Differential reflectivity vs d_M for the garnet-based design shown ($Q_2 - Q_1$)

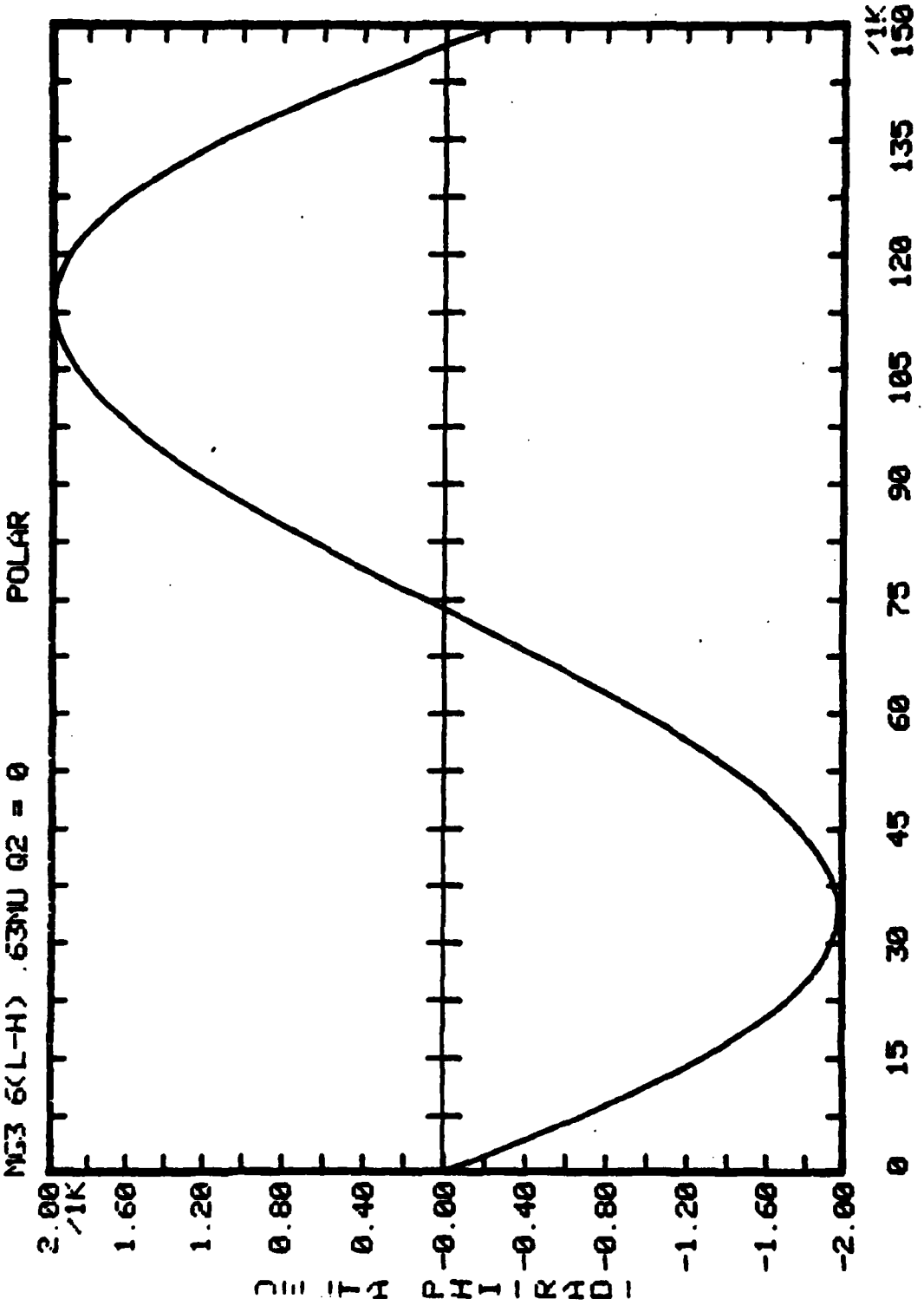

Figure 19 — Differential phase shift vs d_M for the garnet-based design shown

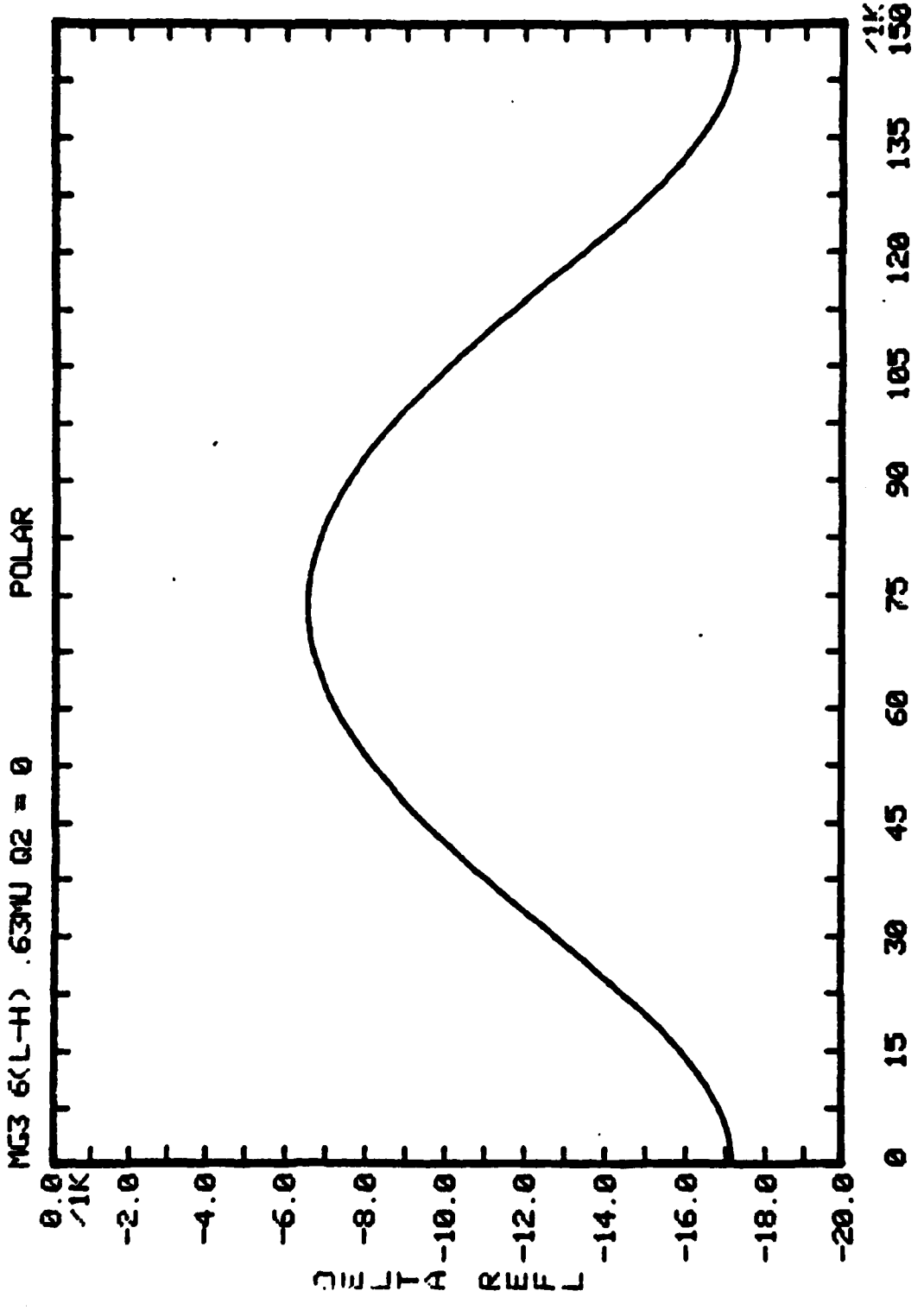

Figure 20 — Differential reflectivity vs d_M for the garnet-based design shown

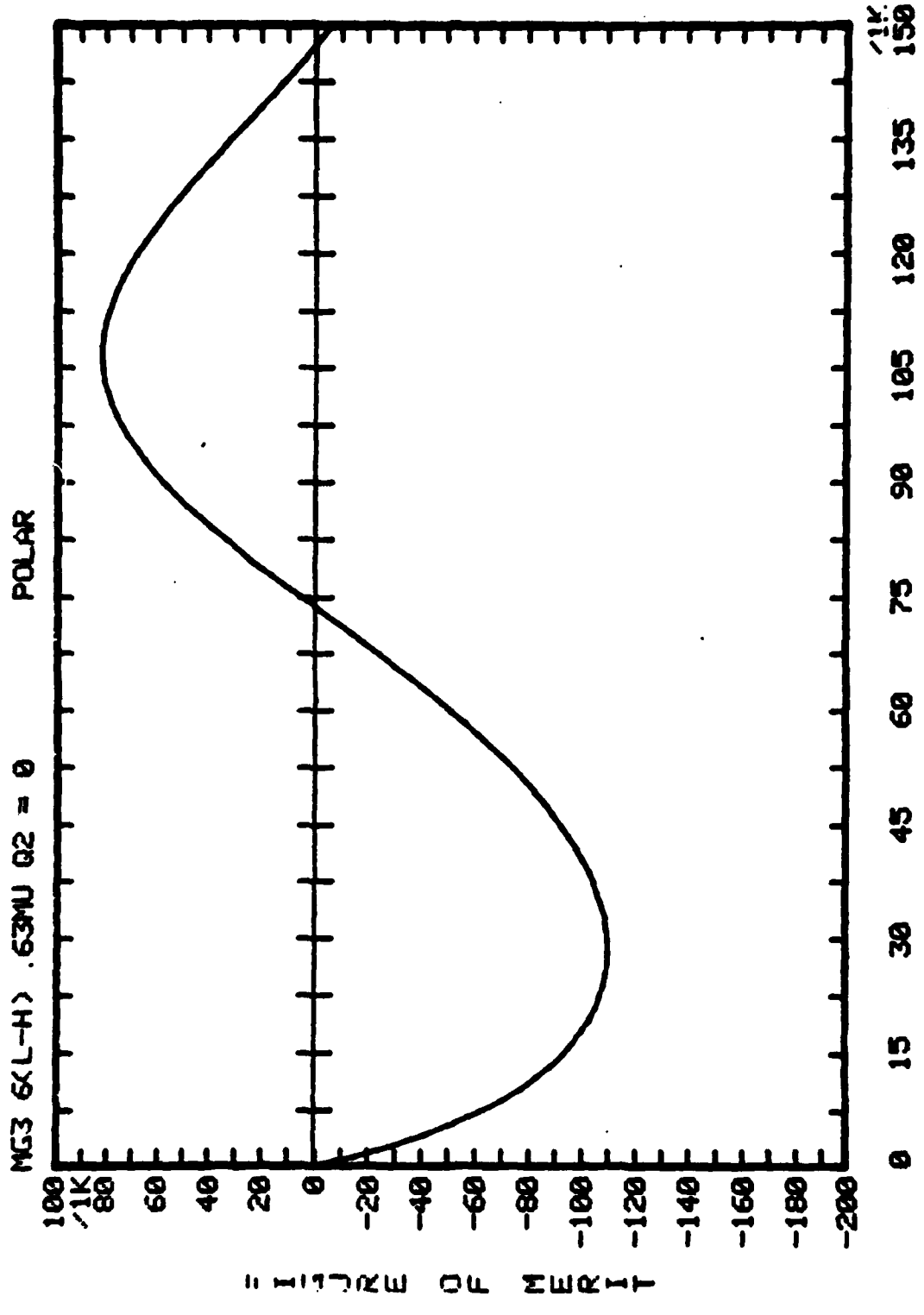

Figure 21 — Figure of merit vs d_M for the garnet-based design shown

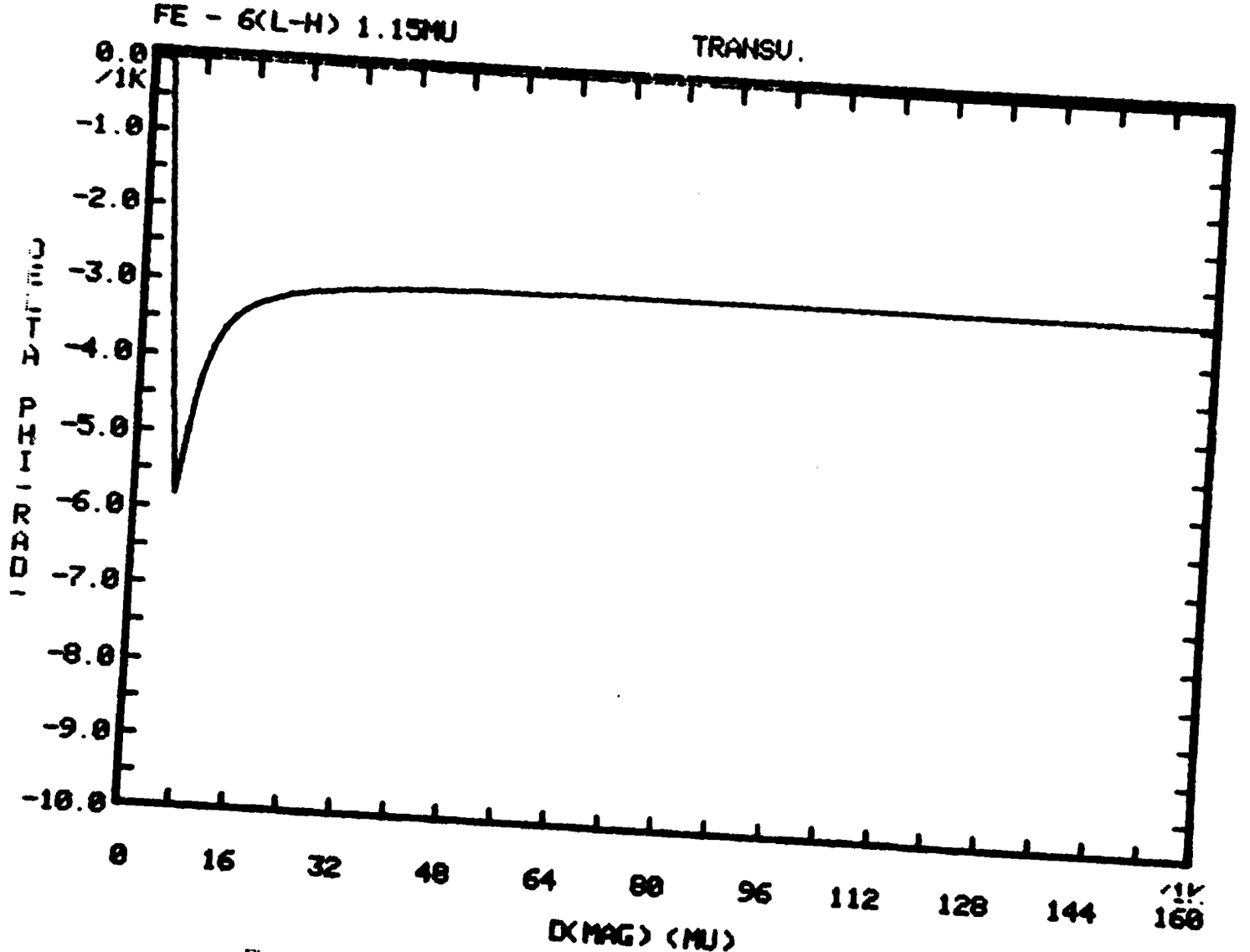

Figure 22 — Differential phase shift vs d_M for the Fe-based design shown

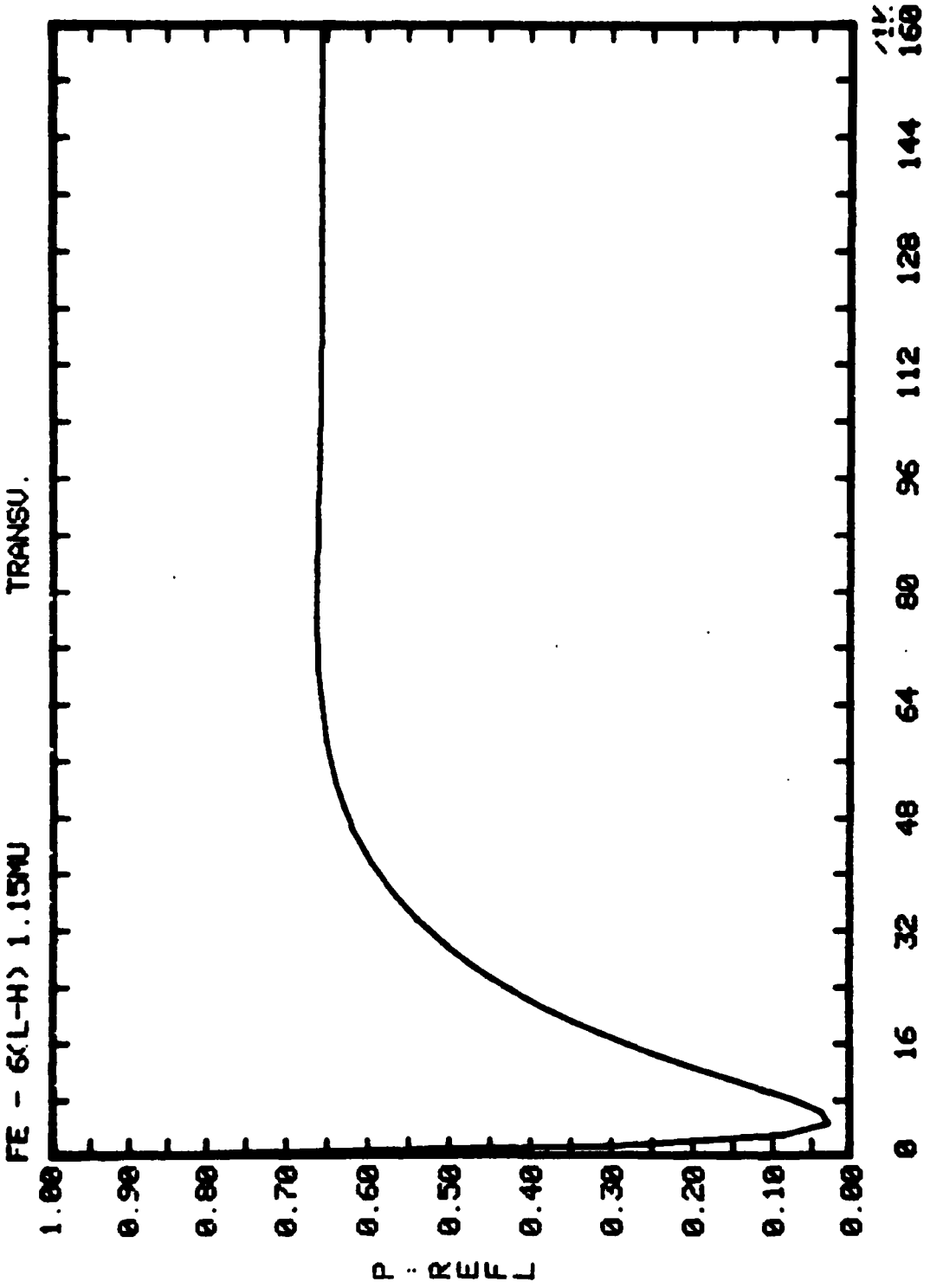

Figure 23 — Reflectivity vs d_M for the Fe-based design shown

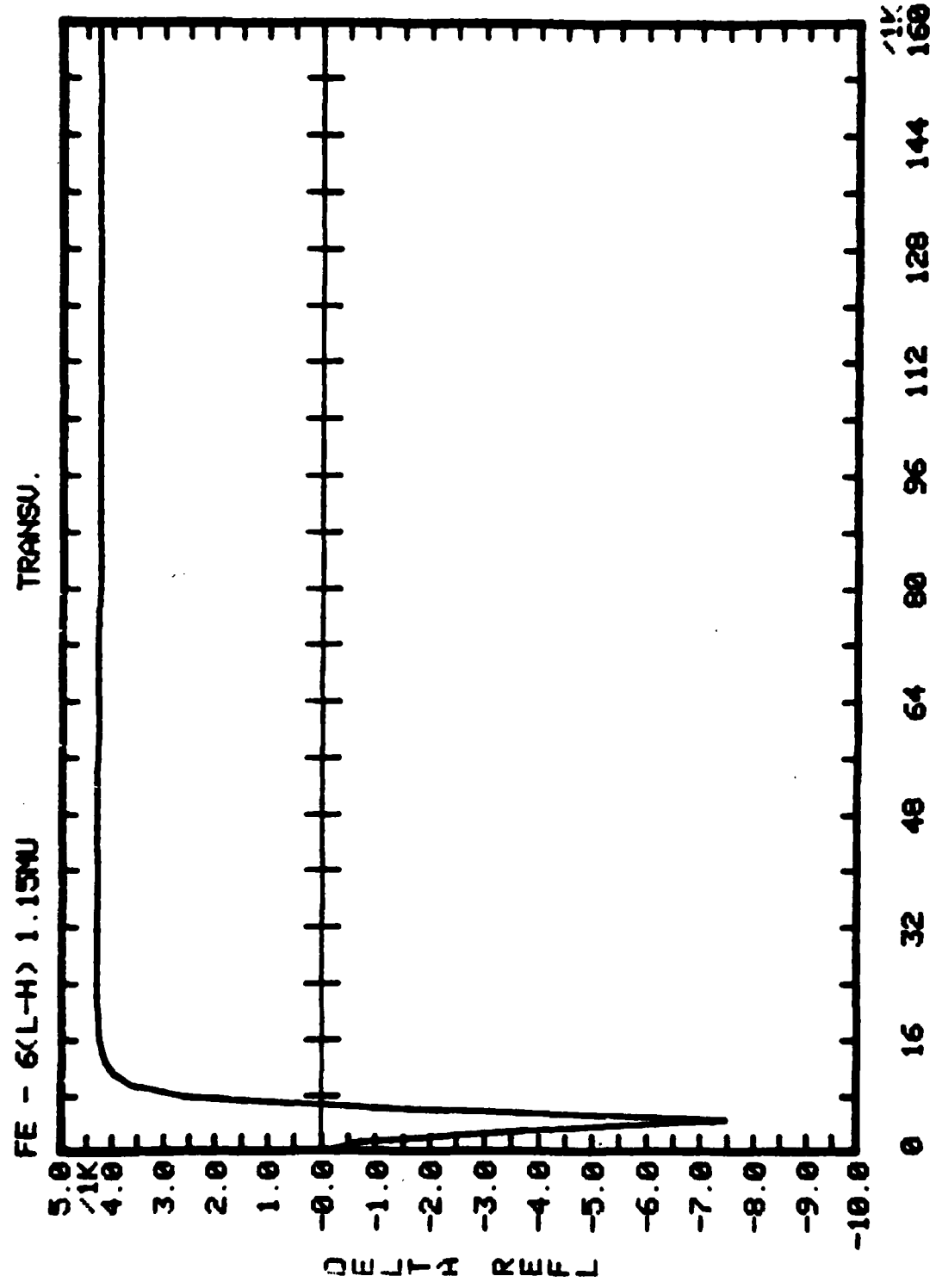

Figure 24 — Differential reflectivity for the Fe-based design shown

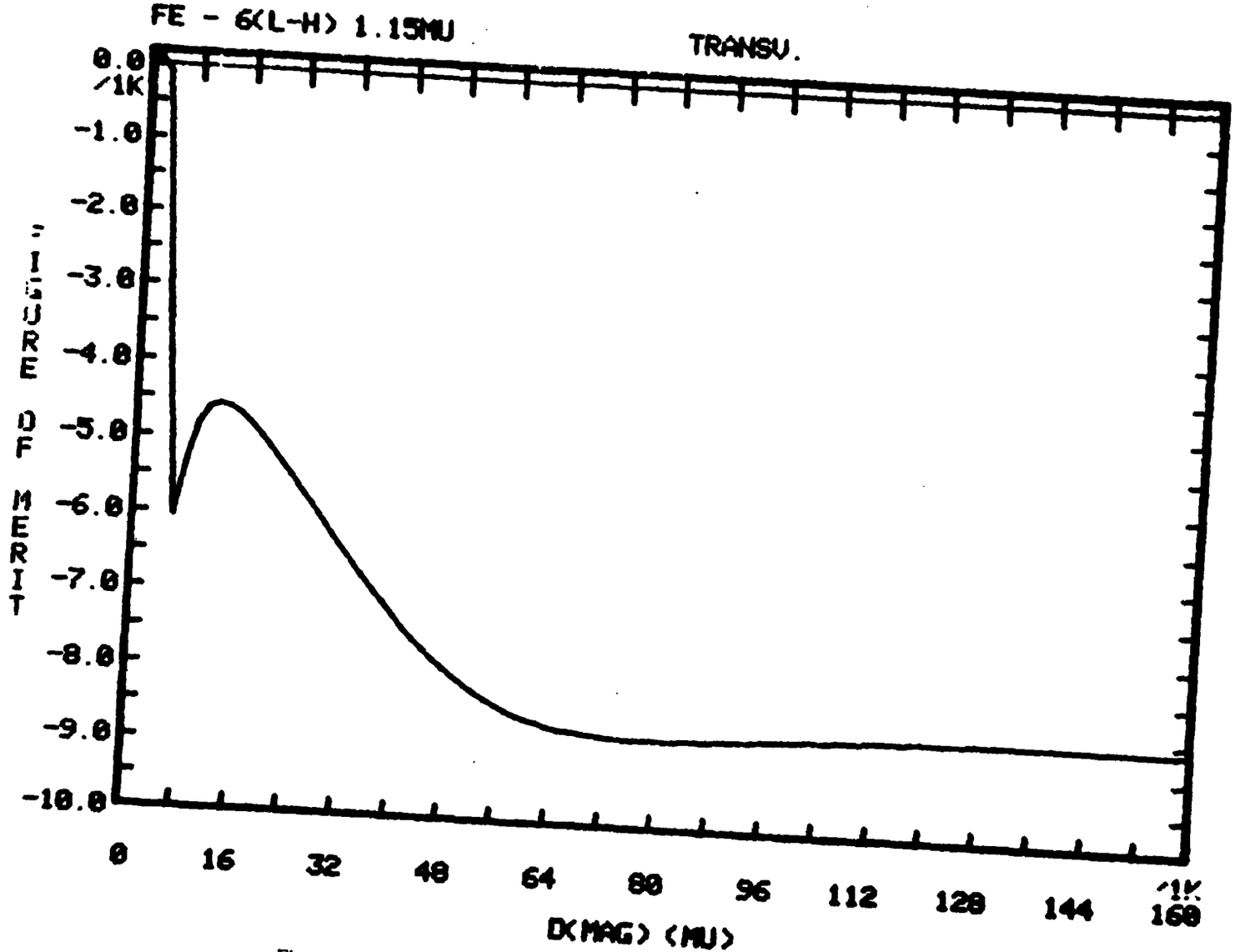

Figure 25 — Figure of merit vs d_M for the Fe-based design shown